

1 **Export fluxes of dissolved inorganic carbon to the Northern Indian Ocean**
2 **from the Indian monsoonal rivers**

3
4 Moturi S. Krishna¹, Rongali Viswanadham¹, Mamidala H. K. Prasad¹, Vuravakonda R.
5 Kumari¹, Vedula V. S. S. Sarma¹

6 ¹CSIR-National Institute of Oceanography, Regional Centre, Visakhapatnam, 530017, India

7
8 *Correspondence to:* M. S. Krishna (moturi@nio.org)
9

10 **Abstract.** Rivers are an important source of dissolved inorganic carbon (DIC) to the adjacent
11 coastal waters. In order to examine the spatial variability in the distribution and major
12 sources of DIC in the Indian monsoonal rivers and to quantify their export flux to the north
13 Indian Ocean, 27 major and medium rivers were sampled during the discharge period.
14 Significant spatial variability in concentrations of DIC (3.4 – 73.6 mg l⁻¹) was observed and it
15 is attributed to spatial variations in the precipitation pattern, size of rivers, pollution, and
16 lithology of the catchments. The stable isotopic composition of DIC ($\delta^{13}\text{C}_{\text{DIC}}$) also showed
17 strong spatial variability (-13.0 to -1.4‰) in the Indian monsoonal rivers with relatively
18 depleted $\delta^{13}\text{C}_{\text{DIC}}$ values in rivers of the northwestern of India (-11.1±2.3‰) and enriched
19 values in the southeastern India (-3.5±2.3‰). Results of the least square linear regression
20 models of Keeling and Miller-Tans plots indicated that chemical weathering of carbonate and
21 silicate minerals by soil CO₂ is the major source of DIC in the Indian monsoonal rivers.
22 Spatial variability in the deviation of $\delta^{13}\text{C}_{\text{DIC}}$ from the approximated $\delta^{13}\text{C}$ of source may
23 probably due to dominant autotrophic production in rivers of the southeast region whereas,
24 heterotrophic decomposition of organic matter largely influences in the other Indian
25 monsoonal rivers. It is estimated that the Indian monsoonal rivers annually export ~10.3 Tg
26 of DIC to the northern Indian Ocean, of which the major fraction (75%) enters into the Bay of
27 Bengal and the remaining reaches to the Arabian Sea. This is consistent with the freshwater
28 flux which is three times higher to the Bay of Bengal (~378 km³ yr⁻¹) than to the Arabian Sea
29 (122 km³ yr⁻¹). Despite discharge from the Indian monsoonal rivers account for only 1.3%

30 of the global freshwater discharge, they disproportionately export 2.5% of the total DIC
31 export by the world major rivers. Despite rivers from the SW region of India export an order
32 of magnitude lower DIC (0.3 Tg yr^{-1}) than the rivers from other regions of India, the highest
33 yield of DIC was found in the former and it is attributed to intense precipitation ($\sim 3000 \text{ mm}$),
34 favorable natural vegetation of tropical moist deciduous and tropical wet evergreen and semi-
35 evergreen forests, tropical wet climate, high soil organic carbon and the dominance of red
36 loamy soils in catchments of the rivers from SW region.

37 *Keywords:* dissolved inorganic carbon, export flux, Indian rivers, Bay of Bengal, Arabian
38 Sea, North Indian Ocean

39 **1. Introduction**

40 Dissolved inorganic carbon (DIC) is one of the major constituent of carbon species in
41 rivers. DIC in rivers mainly originates from the geogenic (weathering of carbonate and
42 silicate rocks) and biogenic (decomposition of organic matter in soils) sources (Meybeck,
43 1987; Mook and Tan, 1991; Gaillardet et al., 1999, Dessert et al., 2001; Viers et al., 2007;
44 Raymond et al., 2008; Tamooh et al., 2013). The former consumes atmospheric carbon
45 dioxide (CO_2) while the latter releases CO_2 fixed by the terrestrial plants. In addition to these
46 major sources in the catchment, DIC is also contributed by various physical and biological
47 processes within the rivers. For instance, heterotrophic decomposition of organic matter,
48 photo-oxidation of dissolved organic carbon (DOC), autotrophic respiration and dissolution
49 of atmospheric CO_2 contribute DIC to rivers. On the other hand, autotrophic production by
50 aquatic plants (photosynthesis) and evasion of CO_2 to atmosphere with draw DIC from rivers.
51 All these processes in the catchments and within the rivers are strongly coupled to
52 atmospheric CO_2 because they act as either sink or source of atmospheric CO_2 (e.g. Berner et
53 al., 1983; Mook and Tan, 1991; Gaillardet et al., 1999; Richey et al., 2002). The DIC in

54 rivers and its export to the coastal oceans is thus intimately linked to the global carbon cycle
55 (Campeau et al., 2017)

56 Riverine export fluxes of DIC to coastal regions of the world oceans have been
57 estimated on the global (Gaillardet et al., 1999) and regional scales (Richey et al., 2002;
58 Wallin et al., 2013; Crawford et al., 2014; Campeau et al., 2014; Kokic et al., 2015) to
59 understand the component of DIC in the global carbon budget. Annual export flux of DIC
60 from the world major river systems to the global ocean has been estimated as ~327 - 385 Tg
61 ($1\text{Tg}=10^{12}\text{g}$) (Ludwig et al., 1998; Meybeck and Vorosmarty, 1999). However, many of the
62 regional studies on DIC export fluxes were limited only to the major river systems (e.g.
63 Gaillardet et al., 1999; Joesoef et al., 2017), for example, the Mississippi (Raymond and
64 Cole, 2003; Raymond et al., 2008; Cai et al., 2008), Changjiang and Pearl (Cai et al., 2008)
65 and Congo (Wang et al., 2013) rivers etc. Regional studies on the riverine export fluxes of
66 DIC are very important for the global carbon cycle and budget as the export fluxes are largely
67 dependent on the hydrological, lithological and environmental conditions, which are highly
68 variable on the regional scales. However, DIC measurements are still lacking in several
69 medium rivers from different regions of the world in general and Asia in particular.

70 Studies on the sources and export fluxes of DIC from the Indian rivers are very
71 limited. Though DIC measurements were conducted in some Indian estuaries, for example,
72 Mandovi and Zuari (Sarma et al., 2001), Godavari (Sarma et al., 2011), Cochin (Gupta et al.,
73 2009; Bhavya et al., 2018), Hooghly (Mukhopadhyay et al., 2002; Samanta et al., 2015),
74 Mahanadi (Pattanaik et al., 2017) and Chilka (Gupta et al., 2008; Muduli et al., 2013), they
75 were confined only to the internal cycling of DIC and exchange of CO_2 at the air-water
76 interface, but not focused on the sources and export fluxes of DIC. The major sources of DIC
77 in the Indian rivers remain unclear, except only a couple of rivers, Krishna (Das et al., 2005;
78 Laskar et al., 2014) and Ganges (Samanta et al., 2015). Further, the quantity of annual DIC

79 export by the Indian rivers to the coastal regions is unknown. Here, we made an attempt to
80 understand the major sources of DIC in the Indian monsoonal rivers (Fig. 1) using $\delta^{13}\text{C}_{\text{DIC}}$ as
81 a potential tracer, and to estimate the riverine export flux of DIC to the north Indian Ocean
82 from the Indian subcontinent.

83 The stable isotopic composition of DIC ($\delta^{13}\text{C}_{\text{DIC}}$) is widely used to identify the major
84 sources of DIC in the aquatic systems (e.g. Singh et al., 2005; Tamooch et al., 2013; Samanta
85 et al., 2015; Zou, 2016). The isotopic composition of DIC originated by dissolution of
86 atmospheric CO_2 is about 0‰ (Coplen et al., 2002) whereas it is about -27 to -26‰ if the
87 DIC is derived from oxidation of organic matter produced by C_3 plants (O’Leary, 1988). The
88 $\delta^{13}\text{C}$ of DIC generated by carbonic acid (formed by soil CO_2 dissolution) weathering of
89 silicates is about -21 to -17‰ (Solomon and Cerling, 1987) while it is in the range of -10 to -
90 9‰ for carbonate rocks because half of the carbon comes from carbonate rocks (0‰, Land,
91 1980) during weathering. The weathering of silicate and carbonate minerals yield $\delta^{13}\text{C}_{\text{DIC}}$ in
92 the range of -8 to -7‰ and -4 to -3‰, respectively, if the carbonic acid formed by the
93 dissolution of atmospheric CO_2 . Though the $\delta^{13}\text{C}$ of DIC derived from different sources is
94 well separable (Deines et al., 1974), the isotopic fractionation by in-stream physical and
95 biological processes alters the $\delta^{13}\text{C}$ of DIC source (Fig. 2). For example, photosynthesis and
96 degassing enriches (O’Leary, 1988; Finlay, 2004; Parker et al., 2005, 2010; Polsenaere and
97 Abril, 2012; Venkiteswaran et al., 2014) while the heterotrophic decomposition of organic
98 matter and photo-oxidation of dissolved organic carbon depletes the $\delta^{13}\text{C}$ of DIC (Opsahl and
99 Zepp, 2001; Finlay, 2003; Waldron et al., 2007; Vahatalo and Wetzel, 2008) (Fig. 2).
100 Though, rivers are generally in disequilibrium with atmospheric CO_2 (Raymond et al., 2013)
101 and emit CO_2 to atmosphere due to oversaturation (Oquist et al., 2009; Campeau et al., 2017),
102 the isotopic equilibration between the DIC and CO_2 in the atmosphere significantly influences
103 the $\delta^{13}\text{C}_{\text{DIC}}$ in rivers (Abongwa and Atekwana, 2014; Deirmendjian and Abril, 2018) due to

104 selective fluxes of $^{12}\text{CO}_2$ and $^{13}\text{CO}_2$ at the water-air interface. Hence, the influence of
105 biogeochemical processes within the rivers must be considered while interpreting the $\delta^{13}\text{C}_{\text{DIC}}$
106 results for identification of DIC sources. The main objectives of this study are to (i) identify
107 the major sources of DIC in the Indian monsoonal rivers, (ii) estimate the export flux and
108 yield of DIC to the north Indian Ocean and (iii) examine the major processes in the
109 catchments and within the rivers controlling DIC in the Indian monsoonal rivers.

110 **2. Study region, sampling and methods**

111 **2.1 Study Area**

112 The Indian peninsula bifurcates the north Indian Ocean into the Bay of Bengal and the
113 Arabian Sea. Although these two basins occupy the same latitudinal belt, their
114 oceanographic processes were reported to be remarkably different due to higher freshwater
115 flux into the Bay of Bengal ($1.63 \times 10^{12} \text{ m}^3 \text{ yr}^{-1}$) than to the Arabian Sea ($0.3 \times 10^{12} \text{ m}^3 \text{ yr}^{-1}$;
116 Subramanian, 1993; Gauns et al., 2005). The large freshwater influx leads to the formation
117 of a strong vertical salinity stratification in the Bay of Bengal (Varkey et al., 1996) that
118 prevents vertical mixing of nutrient rich sub-surface water with the surface (Prasanna Kumar
119 et al., 2004). As a result, the Bay of Bengal is considered to be relatively less productive
120 (Prasannakumar et al., 2002) than the adjacent Arabian Sea, which is one of the highly
121 productive zones in the world (Madhupratap et al., 1996; Smith, 2001; Barber et al., 2001)
122 due to injection of nutrients into the surface through the seasonal upwelling and convective
123 mixing (Shetye et al., 1994; Madhupratap et al., 1996; Muraleedharan and Prasannakumar,
124 1996).

125 Discharge from the Indian monsoonal rivers is largely fed by the monsoon induced
126 precipitation over the Indian subcontinent, which receives >80% of its annual rainfall during
127 the southwest (SW) monsoon period (June-September) (Soman and Kumar, 1990). Though
128 some amount of rainfall occurs during the northeast (NE) monsoon (December-March), it

129 does not generate discharge as it will be stored within the dam reservoirs for domestic,
130 industrial and irrigation purposes. Discharge from the Indian monsoonal rivers mainly occurs
131 during the SW monsoon season (Vijith et al., 2009; Sridevi et al., 2015) hence, these rivers
132 are called as monsoonal rivers. Since the major portion of the annual freshwater discharge
133 occurs only during the SW monsoon, the entire estuary is filled with freshwater (Vijith et al.,
134 2009; Sridevi et al., 2015) during this period. As discharge is small during the rest of the
135 year, the discharge during the SW monsoon (wet period) is considered to be equivalent to the
136 annual discharge of the monsoonal rivers. Based on rainfall intensity, forest cover, vegetation
137 and soil type in the catchment, rivers sampled in the present study were categorized into 4
138 groups, namely the northwest (NW), southwest (SW), southeast (SE) and northeast (NE)
139 rivers of India (Fig. 1). The SW region of India is characterized by the intense rainfall during
140 SW monsoon (~3000 mm) following the NE (1000-2500 mm), SE (300-500 mm) and NW
141 (200-500 mm) regions of India (Soman and Kumar, 1990). The SW rivers drain red loamy
142 soils while the NW rivers drain black soils. Except the major rivers Godavari and Krishna,
143 all the rivers reaching Bay of Bengal (NE and SE rivers) drain red loamy and alluvial soils in
144 their upper and lower catchments respectively. The Godavari and Krishna rivers drain black
145 soils in their upper catchment whereas red loamy and alluvial soils in their middle and lower
146 catchments respectively (Geological Survey of India; www.gsi.gov.in). Based on discharge,
147 the monsoonal rivers in this study were divided into two types, namely, the major ($>150 \text{ m}^3 \text{ s}^{-1}$)
148 ¹) and medium ($<150 \text{ m}^3 \text{ s}^{-1}$) rivers.

149 **2.2 Sample collection**

150 Water samples were collected from the freshwater regions of the estuaries to obtain
151 reliable export fluxes of DIC to the coastal ocean. Samples were collected at 2 to 3 locations
152 to minimize the spatial variability within the freshwater zone of the estuary. Further, to
153 minimize the inter-annual variability in DIC concentrations, sampling was conducted in two

154 different years and the mean was used for export flux estimations. Further, samples were
155 collected in mid-stream of the river using a local mechanized boat to avoid the contamination
156 from river banks.

157 *In-situ* measurements and sample collection were conducted in 27 rivers of the Indian
158 subcontinent (Fig. 1) during the SW monsoon season of the years, 2011 and 2014. Surface
159 water samples at each location were collected for phytoplankton biomass (Chl-*a*), DIC and
160 dissolved oxygen (DO). Samples for DIC were collected in air-tight crimp-top glass bottles
161 and added poison (mercuric chloride) to arrest the biological activity. DO analysis was
162 carried out at a temporary shore laboratory set up for sample processing after the completion
163 of sampling on each day. Water samples were filtered through GF/F (nominal pore size of
164 0.7 μ m) under moderate vacuum and stored in liquid nitrogen for Chl-*a* analysis.

165 **2.3. Methods**

166 Temperature and salinity at the sampling locations were measured using a
167 conductivity-temperature-density (CTD) profiling system (Sea Bird Electronics, SBE 19 plus,
168 United States of America). Concentration of DO was determined by a Winkler's method
169 (Carritt and Carpenter, 1966) using an auto titrator (Metrohm, Switzerland) with
170 potentiometric end point detection. The analytical precision of the method was $\pm 0.07\%$
171 (RSD). Dissolved oxygen saturation is computed following formulations given by Garcia and
172 Gordon (1992). DIC concentrations in water samples were measured at our Institute
173 laboratory using Coulometer (UIC Inc., USA) connected to an automatic sub-sampling
174 system. Based on the repeated analysis of samples and standards, the precision of the method
175 was $\pm 0.02 \text{ mg l}^{-1}$. The certified reference materials (CRM) supplied by Dr. A.G. Dickson,
176 Scripps Institute of Oceanography, USA and internal standards were used to test the accuracy
177 of our DIC measurements and it was found to be within ± 0.2 to 0.3% . Potentiometric Gran
178 titration method (Metrohm, Switzerland) was used for determination of pH and total

179 alkalinity and followed the standard operating procedures given by Department of Energy
180 (DOE) (1998).

181 The stable carbon isotopic composition of DIC in the water was measured on Gas
182 Bench coupled with isotope ratio mass spectrometer (EA-IRMS-Delta V,
183 Finnigan, Germany). 50 ml air-tight bottles with rubber septa were filled with 0.5 ml of high
184 purity ortho-phosphoric acid and purged with high purity helium. About 1 ml of water sample
185 is injected to the bottle and incubated at constant temperature of 50°C for 12 hours. The CO₂
186 extracted into the head space is injected to the IRMS through gas bench. The results are
187 expressed relative to conventional standards, that is, Pee Dee Belemnite (PDB) limestone for
188 carbon (Coplen, 1996) as δ values, defined as:

$$\delta R = [(X_{\text{sample}} - X_{\text{standard}}) / X_{\text{standard}}] \times 10^3 \text{ ‰}$$

189
190 where R refers to ¹³C and X stands for ¹³C/¹²C. The high-purity tank of CO₂ was used as
191 working standard for carbon. These gases were calibrated with IAEA standards. Standard
192 deviation on 20 aliquots of the same sample was lower than 0.05‰ for δ¹³C. Chlorophyll-*a*
193 (Chl-*a*) on the filter was extracted into di-methyl formamide (DMF) and measured the extract
194 fluorometrically using a spectrofluorophotometer (Varian Eclipse, Varian Electronics., UK)
195 following Suzuki and Ishimaru (1990). Annual mean discharge data of the rivers was taken
196 from Meybeck and Ragu (1995, 1996), Central Water Commission, New Delhi (2006, 2012)
197 and Kumar et al. (2005). Catchment area of the rivers was obtained from Water Resources
198 Information System of India (WRIS, www.india-wris.nrsc.gov.in). Soil organic carbon data
199 was taken from Kishwan et al. (2009) and Sreenivas et al. (2016), and the rainfall data was
200 obtained from Soman and Kumar (1990). Dissolved organic carbon (DOC) data for the
201 Indian rivers was taken from Krishna et al. (2015)

202
203 Total export flux of DIC from each river was estimated by multiplying the mean
204 concentrations of DIC at near zero salinity (river end member) with the annual discharge.

205 Spatial variability of DIC concentrations within the river was minimized to a large extent by
206 collecting samples from 2 to 3 locations in each river while the inter-annual variability by
207 collecting samples during discharge periods of two years. However, variability in DIC
208 concentrations within the discharge period results in some uncertainties in our estimations of
209 DIC export fluxes. Time series measurements in the Godavari estuary (our unpublished
210 results) revealed that the variability in DIC concentrations within the discharge period is up to
211 10%. Therefore, the error associated with our DIC flux estimates may be about 10%. DIC
212 flux normalized by catchment area (yield) was calculated by dividing the total DIC export
213 flux of the river by its catchment area.

214 **3. Results**

215 **3.1. Hydrographic characteristics**

216 Surface water temperatures were higher in rivers from the NE and SE regions (mean
217 $30.9 \pm 1.2^\circ\text{C}$) than the rivers from SW and NW regions ($27.3 \pm 1.5^\circ\text{C}$) of India. Dissolved
218 oxygen saturation varied from as low as 63% to as high as 105%, with a mean saturation of
219 $90 \pm 11\%$. The rivers from SW region of India recorded more under-saturation of DO ($82 \pm 7\%$)
220 than the rivers located in the NE ($89 \pm 15\%$), NW ($93 \pm 3\%$) and SE ($96 \pm 11\%$) regions of India.
221 Chlorophyll-*a* (Chl-*a*) concentrations varied broadly from 0.8 to 7.5 mg m^{-3} , with relatively
222 higher mean concentrations in rivers of the SE region ($4.7 \pm 2.5 \text{ mg m}^{-3}$) followed by the SW
223 ($2.8 \pm 0.7 \text{ mg m}^{-3}$) regions of India. On the other hand, relatively low Chl-*a* was observed in
224 the medium ($2.6 \pm 1.3 \text{ mg m}^{-3}$) than the major estuaries ($3.2 \pm 2.1 \text{ mg m}^{-3}$).

225 **3.2 DIC concentrations and $\delta^{13}\text{C}_{\text{DIC}}$**

226 DIC concentrations in the Indian monsoonal rivers widely varied from 3.4
227 (Bharathapuzha) to 73.6 mg l^{-1} (Vellar), with a significant spatial variability (Fig. 3a; Table
228 1). Highest mean DIC concentration was observed in rivers of the SE region ($37.4 \pm 6.3 \text{ mg l}^{-1}$)
229 while the lowest was found in the SW region ($5.2 \pm 2.1 \text{ mg l}^{-1}$) of India. Intermediate values

230 were found in rivers of the NW ($28.4 \pm 8.9 \text{ mg l}^{-1}$) and NE ($17.1 \pm 6.2 \text{ mg l}^{-1}$) regions of India.
231 DIC concentrations were found to be similar in the major ($22.7 \pm 13.6 \text{ mg l}^{-1}$) and medium
232 ($21.1 \pm 13.2 \text{ mg l}^{-1}$) rivers (homoscedastic Student's t-test; $p=0.76$). Mean DIC concentration
233 found in this study ($21.4 \pm 16.3 \text{ mg l}^{-1}$) is similar to those observed earlier in the major river
234 systems of India (Brahmaputra; Singh et al., 2005) and elsewhere in the world, for example,
235 British rivers (Jarvie et al., 2017) and Swedish rivers (Campeau et al., 2017). However, DIC
236 concentrations in the present study are higher than the global mean DIC (10.3 mg l^{-1} ,
237 Meybeck and Vorosmarty, 1999) (Table 1), but lower than those reported in the rivers
238 draining into the Gulf of Trieste (N Adriatic; $37\text{-}66 \text{ mg l}^{-1}$, Tamse et al., 2014).

239 The $\delta^{13}\text{C}_{\text{DIC}}$ varied from -13.0 to -1.4‰ , with a significant spatial variability (Fig. 3d;
240 Table 1) in the rivers sampled. Relatively depleted $\delta^{13}\text{C}_{\text{DIC}}$ values were observed in rivers of
241 the NW region ($-11.1 \pm 2.3\text{‰}$) while enriched $\delta^{13}\text{C}_{\text{DIC}}$ was found in rivers of the SE region ($-$
242 $3.5 \pm 2.3\text{‰}$) of India (Fig. 3d). The $\delta^{13}\text{C}_{\text{DIC}}$ values found in this study are well within the range
243 of values reported earlier in rivers of India (Das et al., 2005) and elsewhere in the world, for
244 example, Swedish streams (-27.6 to -0.6‰ ; Campeau et al., 2017) and rivers from Italy and
245 Slovenia (-12.8 to -7.7‰ , Tamse et al., 2014).

246 **3.3. Export fluxes and yield of DIC**

247 Annual export flux of DIC to the coastal ocean from the individual rivers varied
248 broadly from 0.01 Tg (Chalakkudi) to as high as 2.33 Tg (Krishna) (Fig. 3b; Table 1). Among
249 the rivers sampled, rivers of the NE region of India export higher DIC (6.52 Tg yr^{-1}) while
250 the lowest was found from rivers of the SW region (0.24 Tg yr^{-1}) (Table 1). The Indian
251 monsoonal rivers together export about 10.32 Tg yr^{-1} of DIC to the northern Indian Ocean, of
252 which 7.81 Tg (75%) enters into the Bay of Bengal and the remaining into the Arabian Sea
253 (2.51 Tg). The yield of DIC ranged from 2.8 (Bharathapuzha) to $20.7 \text{ g m}^{-2} \text{ yr}^{-1}$ (Baitarani)
254 (3c ; Table 1), excluding the exceptionally high yield of $119 \text{ g m}^{-2} \text{ yr}^{-1}$ from Haldia river. The

255 mean yield was found to be more or less similar in rivers from all the four regions of India,
256 i.e, NW ($8.4 \text{ g m}^{-2} \text{ yr}^{-1}$), SW ($8.8 \text{ g m}^{-2} \text{ yr}^{-1}$), SE ($6.6 \text{ g m}^{-2} \text{ yr}^{-1}$) and NE ($7.7 \text{ g m}^{-2} \text{ yr}^{-1}$)
257 regions. Despite the export flux of DIC is lowest from rivers of the SW region (0.24 Tg yr^{-1}),
258 interestingly, the yield from rivers of this region is on par with (even slightly higher than) the
259 other Indian monsoonal rivers (Table 1; Fig. 3b&c). Yields of DIC found in this study are
260 similar to those found earlier in rivers elsewhere in the world (Huang et al., 2012).

261 4. Discussion

262 4.1 Distribution of DIC in the Indian monsoonal rivers

263 Distribution of DIC in the Indian monsoonal rivers showed large spatial variability,
264 with the lowest values in rivers from the SW region of India (Fig. 3a). DIC concentrations in
265 rivers are known to be influenced by the intensity of precipitation over the catchment, basin
266 lithology (Giesler et al., 2013; Lofgren et al., 2014), length of the fluvial network (Hotchkiss
267 et al., 2015) and in-stream physical and biological processes (Mook and Tan, 1991; Raymond
268 et al., 2008). The spatial distribution of rainfall over the Indian subcontinent
269 (www.imd.gov.in) shows that the SW region receives the highest annual rainfall ($\sim 3000 \text{ mm}$)
270 than the rest of India (Soman and Kumar, 1990).

271 The intense precipitation over the SW region is expected to cause higher weathering
272 rates and thus higher DIC in rivers (e.g., Gupta et al., 2011), but lower DIC concentrations
273 were found in rivers of this region. It could be due to the influence of dilution because the
274 dense precipitation over the small catchment area (Table 1) might have diluted DIC
275 concentrations in rivers of this region. In order to understand the influence of the density of
276 rainfall on DIC in rivers, we normalized the volume of discharge from the river with its
277 catchment area. The catchment area normalized volume of discharge was found to be much
278 higher in rivers from the SW region ($1.71 \text{ m}^3 \text{ m}^{-2}$) than the rivers from SE ($0.17 \text{ m}^3 \text{ m}^{-2}$), NE
279 ($0.6 \text{ m}^3 \text{ m}^{-2}$) and NW ($0.32 \text{ m}^3 \text{ m}^{-2}$) regions of India. About three times higher catchment

280 area normalized discharge might have diluted DIC concentrations in the rivers of the former
281 region. A strong exponential decrease in DIC concentrations with increasing rainfall over the
282 catchment ($r^2= 0.72$, $p<0.001$; Fig. 4a) also suggests that DIC concentration in the Indian
283 rivers are strongly influenced by density of precipitation over the catchment.

284 Rivers of the SW region are relatively small in size, both in terms of catchment area
285 (total catchment area: $20 \times 10^3 \text{ km}^2$) and the length of the river (mean length: 126 km), than
286 the rivers from other regions (SE, NE and NW) of India (Table 1). Since the contribution of
287 DIC from in-stream processes, such as decomposition of organic matter, has been
288 demonstrated to increase along the course of the fluvial network (Hotchkiss et al., 2015),
289 possibly due to increase in the residence time of water (Catalan et al., 2016), the lowest DIC
290 concentrations found in rivers from the SW region may also, at least partly, be due to their
291 small size. Fairly good positive correlation between DIC concentrations and length of the
292 rivers ($r^2=0.38$, $p<0.01$; Fig. 4b) also support this argument.

293 The major physical and biological processes controlling DIC concentrations in rivers
294 are the exchange of CO_2 with the atmosphere, autotrophic removal and heterotrophic
295 addition of DIC. Since the Indian monsoonal estuaries have been reported to be a source of
296 CO_2 to the atmosphere during the discharge period due to heterotrophic decomposition of
297 organic matter (Sarma et al., 2001, 2011, 2012; Gupta et al., 2008, 2009; Bhavya et al.,
298 2018), the DIC input from the dissolution of atmospheric CO_2 may be unlikely. On the other
299 hand, organic matter decomposition is expected to add significant amount of DIC as
300 enhanced bacterial respiration rates were reported during this period (Sarma et al., 2011;
301 2012). In contrast, significant negative correlation between chlorophyll-*a* and DIC ($r^2=-0.44$,
302 $p<0.01$; Fig. 4c), except few SE rivers where elevated phytoplankton biomass (Chl-*a*: $>5 \text{ mg}$
303 m^{-3}) was recorded, suggesting that autotrophic removal of DIC is also significant in the
304 Indian monsoonal rivers during the study period. A significant positive relationship was

305 observed between the $\delta^{13}\text{C}_{\text{DIC}}$ and Chl-a ($r^2=0.49$; $p<0.01$; Fig. 4d), supporting this argument
306 because preferential uptake of ^{12}C than ^{13}C during photosynthesis leaves the residual DIC
307 enriched in ^{13}C . On the other hand, $\delta^{13}\text{C}_{\text{DIC}}$ showed significant positive correlation with DO
308 saturation ($r^2=0.50$, $p<0.01$; Fig. 4e) (depleted $\delta^{13}\text{C}_{\text{DIC}}$ values at more under saturation of DO)
309 and DOC concentrations ($r^2=0.43$, $p<0.01$; Fig. 4f) as was observed in the Xi river (Zou et al.,
310 2016). Altogether, enriched $\delta^{13}\text{C}_{\text{DIC}}$ are associated with higher DOC, less under saturation of
311 DO and higher phytoplankton biomass (Chl-a) while the depleted $\delta^{13}\text{C}_{\text{DIC}}$ are associated more
312 under saturation of DO and less DOC. This suggests that both autotrophic removal and
313 heterotrophic addition control DIC in the Indian rivers during the discharge period, with a
314 considerable spatial variability. However, influence of these processes on DIC
315 concentrations is difficult to separate with this bulk $\delta^{13}\text{C}_{\text{DIC}}$ data set, as the $\delta^{13}\text{C}_{\text{DIC}}$ in rivers is
316 also influenced by pollution, catchment lithology and outgassing of CO_2 (Shin et al., 2011;
317 Brunet et al., 2005; Bouillon et al., 2009; Zeng et al., 2011; Tamoooh et al., 2013). Excluding
318 Sabarmati and Mahisagar rivers, DIC concentrations showed fairly good linear relationship
319 with population density over the catchment of the river ($r^2=0.41$, $p<0.01$; Fig. 4g), suggesting
320 that considerable influence of pollution from the mega cities and industries on DIC in the
321 Indian rivers.

322 Spatial distribution of soils shows that rivers of the NW region of India and upper
323 reaches of Krishna and Godavari rivers drain the lime-rich black soils (Fig. 1) while rivers
324 from the SW region drain red loamy soils. Whereas, the east-flowing rivers drain the lime-
325 poor red sandy soils in the upper but lime-rich alluvial soils in the lower reaches (Fig.1).
326 Lateritic soils, which are poor in lime and silicate, occupied the catchment of the rivers in the
327 SW region of India. Relatively lower chemical weathering rates of the lateritic than the non-
328 lateritic soils could be one of the reasons for the observed lower DIC concentration the rivers
329 from SW region of India. A significant positive correlation was found between total

330 alkalinity (TA) and $\delta^{13}\text{C}_{\text{DIC}}$ ($r^2=0.52$; $p<0.01$; Fig. 4h), suggesting that significant contribution
331 of DIC is from weathering of carbonate minerals in the catchment. Though the higher
332 chemical weathering rates were reported for the Deccan Trap basalts (Das et al., 2005;
333 Singh et al., 2005), which occupied the catchments of rivers of the NW region of India and
334 upper reaches of Godavari and Krishna, higher DIC concentrations were also observed in
335 rivers draining over the metamorphic rocks. This suggests that the influences of factors other
336 than bedrock are also significant on the concentrations of DIC in the Indian rivers.

337 **4.2 Major sources of DIC in the Indian monsoonal rivers**

338 Though, the $\delta^{13}\text{C}_{\text{DIC}}$ is a promising tool to decipher the sources of DIC, its
339 interpretation for source material identification in rivers is still challenging because multiple
340 physical and biological processes within the rivers significantly alter the $\delta^{13}\text{C}$ of DIC source.
341 The influence of major in-stream processes on the $\delta^{13}\text{C}_{\text{DIC}}$ must be separated before
342 interpreting the results for major sources of DIC, failing which leads to erroneous
343 conclusions. In order to identify and separate DIC sources, we used here two different
344 graphical mixing model techniques, Keeling plot (Keeling, 1958; Pataki et al., 2003) and
345 Miller-Tans plots (Miller and Tans, 2003). These models approximate the hypothetical $\delta^{13}\text{C}$
346 of source material as an intercept (in Keeling plot) and slope (in Miller-Tans plot) of the least
347 square linear regression equations (Pataki et al., 2003; Campeau et al., 2017). The deviations
348 from the approximated $\delta^{13}\text{C}$ of source can be interpreted as the influence of in-stream
349 processes. Further, we approximated the $\delta^{13}\text{C}$ of CO_2 using a set of enrichment factors of
350 isotopic fractionation across the carbonate species (Zhang et al., 1995) in order to filter the
351 impact of DIC speciation and pH on the bulk $\delta^{13}\text{C}_{\text{DIC}}$ values. This approach has already
352 been used by Quay et al. (1992), Mayorga et al. (2005) and recently by Campeau et al.
353 (2017).

354 Significant negative relationships were observed in both Keeling plot ($\delta^{13}\text{C}_{\text{DIC}}$ as a
355 function of $1/\text{DIC}$; Fig. 5a) and Miller-Tans plot ($\delta^{13}\text{C}_{\text{DIC}} \times \text{DIC}$ as a function of DIC ; Fig.
356 5b) ($r^2=0.61$, $p<0.01$ and $r^2=0.72$, $p<0.01$ respectively) of DIC in the Indian rivers, except the
357 rivers draining the Deccan Trap basalts. Both graphical mixing models, Keeling and Muller-
358 Tans plots, approximated the similar $\delta^{13}\text{C}$ of source material (-3.0‰ and -2.0‰ respectively;
359 Fig. 5a&b), suggesting that weathering of carbonate minerals is the predominant source of
360 DIC in the Indian monsoonal rivers rather than biogenic soil CO_2 . Calculated $\delta^{13}\text{C}$ of CO_2
361 ranged from -21.5 to -9.6‰ in the Indian rivers with a mean value of $-13.0\pm 2.7\text{‰}$. Calculated
362 $\delta^{13}\text{C}$ of CO_2 is linearly correlated with the measured $\delta^{13}\text{C}_{\text{DIC}}$, but correlation coefficient (r^2) is
363 only 0.51 (Fig. 5c), suggesting that significant spatial variability in the influence of in-stream
364 processes on the $\delta^{13}\text{C}_{\text{DIC}}$. The Miller-Tans plot of CO_2 ($\delta^{13}\text{C}\text{-CO}_2 \times \text{CO}_2$ as a function of
365 CO_2) showed highly significant linear regression model with a slope of -10.7‰ ($r^2=0.97$;
366 $p<0.001$; Fig. 5d). These results indicated that chemical weathering of carbonate and silicate
367 minerals by soil CO_2 (-10 to -9‰) is the major source of DIC in the Indian rivers. contributed
368 by. Deviations of the measured $\delta^{13}\text{C}_{\text{DIC}}$ (-13.0 to -1.4‰) from that of the approximated $\delta^{13}\text{C}$
369 of DIC source (-3.0 to -2.0‰) and $\delta^{13}\text{C}$ of CO_2 (-10.7‰) could be due to the influence of in-
370 stream process. In more than 75% of the Indian rivers sampled, the deviation from the $\delta^{13}\text{C}$ of
371 DIC source is towards negative side (depletion) ($\delta^{13}\text{C}_{\text{DIC}} < -3.0\text{‰}$), suggesting that
372 heterotrophic decomposition of organic matter is the dominant process controlling DIC in
373 these rivers. While, no (or very little) deviation was observed only in rivers from the SE
374 region of India (mean $\delta^{13}\text{C}_{\text{DIC}}$: -3.1‰) could be due to the competition between autotrophy,
375 degassing and heterotrophy as these processes influences the $\delta^{13}\text{C}_{\text{DIC}}$ in opposite directions
376 (Fig. 2); the former two processes causes enrichment while the latter depletes $\delta^{13}\text{C}_{\text{DIC}}$.
377 Relatively higher phytoplankton biomass (mean Chl-a : 4.6 mg m^{-3}) and less under-saturation

378 of DO (98.7%) was observed in these rivers compared to the mean of the rest of the Indian
379 rivers (2.4 mg m⁻³ and 87.5% respectively), suggesting that autotrophy is one of the dominant
380 processes controlling DIC in rivers from the SE region of India. Total number of dams on the
381 rivers from this (SE) region (mean 155, Table 1) is not significantly higher from that of the
382 mean of total number of dams on the Indian rivers sampled (mean 135) , suggesting that
383 degassing due to storage of water may not be the dominant process responsible for
384 enrichment in $\delta^{13}\text{C}_{\text{DIC}}$ of these rivers.

385 **4.3 Total DIC export by the Indian monsoonal rivers to the north Indian Ocean**

386 Indian monsoonal rivers annually export ~10.3 Tg of DIC to the north Indian Ocean.
387 Nearly three fourth of this amount (7.8 Tg) reaches to the Bay of Bengal while the Arabian
388 Sea receives only one fourth (2.5 Tg). This is consistent with the higher magnitude of
389 freshwater discharge to the Bay of Bengal (378 km³ yr⁻¹) from the catchment area of about
390 970x10³ km² than the Arabian Sea (122 km³ yr⁻¹ from the catchment area of 244x10³ km²).
391 The total DIC export by the Indian monsoonal rivers (10.3 Tg yr⁻¹) is lower than the DIC
392 export by the American (61.4 Tg yr⁻¹) and African (17.7 Tg yr⁻¹) rivers and major rivers
393 draining to the tropical Atlantic from South America and Africa (53 Tg yr⁻¹, Araujo et al.
394 2014). It is mainly due to the fact that freshwater discharge from the Indian monsoonal rivers
395 is very low (~500 km³ yr⁻¹) compared to the American (11,799 km³ yr⁻¹) and African (3,786
396 km³ yr⁻¹) rivers. However, the Indian monsoonal rivers are exporting disproportionately
397 higher DIC because they account for only 1.3% of the global river discharge but export 2.5%
398 of the global riverine DIC export to the oceans (400 Tg yr⁻¹). Though American and African
399 rivers account for 30% and 10% of the global river discharge, they export only 15% and 4.4%
400 of global riverine DIC to oceans, respectively. Disproportionately higher DIC flux from the
401 Indian rivers could be due to relatively higher weathering rates of silicate and carbonate
402 minerals in their drainage basins (Das et al., 2005; Gurumurthy et al., 2012; Pattanaik et al.,

403 2013). Higher DIC fluxes from the tropical regions are mainly attributed to the favourable
404 climatic conditions, lithology and land use cover (Huang et al., 2012) of this region for higher
405 dissolution.

406 Krishna et al. (2015) reported that Indian monsoonal rivers export 2.32 Tg yr^{-1} of
407 dissolved organic carbon (DOC) to the north Indian Ocean. The total fluvial dissolved carbon
408 flux (DIC+DOC) would be 12.6 Tg yr^{-1} in which DIC flux contributed up to $\sim 81\%$. The
409 predominance of DIC has also been found in rivers elsewhere in the world, for example, the
410 British rivers (Jarvie et al., 2017) and high altitude Swedish rivers (Campeau et al., 2017).
411 Since the catchment area of the Indian monsoonal rivers ranged widely from as low as 1×10^3
412 km^2 to as high as $313 \times 10^3 \text{ km}^2$, the export fluxes of DIC were normalized with the catchment
413 area of the river (yield) in order to examine various factors controlling the DIC export to the
414 north Indian Ocean.

415 **4.4 Yield of DIC from the Indian monsoonal rivers**

416 The yield of DIC found in this study (mean $8.7 \pm 5.2 \text{ g m}^{-2} \text{ yr}^{-1}$) is close to those found
417 in rivers from the tropical region of Asia, but significantly higher than those reported from
418 tropical region of the American and African continents (Huang et al., 2012). The yield was
419 highest ($8.8 \pm 5.6 \text{ g m}^{-2} \text{ yr}^{-1}$) in rivers from the SW region of India, despite they export
420 relatively lower DIC (0.3 Tg yr^{-1}) due to their low volume of discharge ($46 \text{ km}^3 \text{ yr}^{-1}$) and
421 relatively smaller catchment ($20 \times 10^3 \text{ km}^2$) than the rivers from SE, NE and NW regions of
422 India (Table 1. DIC yield showed a significant positive correlation with the volume of
423 discharge ($r^2=0.67$, $p<0.001$; Fig. 6a) in medium rivers and no such relationship was found in
424 the major rivers. Significant negative relationship was observed between DIC yield and
425 catchment area of river ($r^2 = -0.49$, $p<0.001$; Fig. 6b and $r^2 = -0.43$, $p<0.001$; Fig. 6c for
426 medium and major rivers respectively), suggesting the smaller rivers export more DIC per
427 unit area of catchment compared to the major river systems, and thus inclusion of DIC data

428 from medium rivers in the world significantly alters the global estimations of DIC. A fairly
429 good linear relationship between the yield of DIC and the intensity of precipitation ($r^2=0.43$,
430 $p<0.01$ Fig. 6d) was observed only in the rivers which receives $>2000\text{mm}$ of annual mean
431 precipitation. Higher precipitation over the catchment increases the yield of DIC because the
432 dense precipitation enhances the extraction of DIC from soils and rocks in their catchment.
433 Therefore, high precipitation ($\sim 3000\text{ mm}$) over the small catchment ($20 \times 10^3\text{ km}^2$) could have
434 increased DIC yield from the rivers of SW region of India.

435 Sreenivas et al. (2016) and Krishwan et al. (2009) found that the soil organic and
436 inorganic carbon contents in the surface (100cm) soils in the catchment of rivers in the SW
437 region were higher and lower, respectively, than the catchments of the rivers from SE, SW
438 and NE region of India. Decomposition of soil organic matter releases excess CO_2 and, the
439 increase in soil CO_2 leads to the formation of acidic conditions in soils. This would increase
440 the DIC yield by more dissolution of soil carbonates and chemical weathering of carbonate
441 and silicate rocks (Zou et al., 2016). A significant linear correlation was found between soil
442 organic carbon content and DIC yield in this study ($r^2=0.65$, $p<0.001$; Fig. 6e), suggesting
443 that higher soil organic carbon in the catchment of the rivers from SW region could have
444 elevated the yield of DIC from rivers of this region. The basin scale studies are, however,
445 required for comprehensive understanding of the influence of environmental and
446 anthropogenic factors on export fluxes and yield of DIC from the Indian monsoonal rivers.

447 **5. Summary**

448 In order to examine the spatial variability in the sources and distribution of dissolved
449 inorganic carbon (DIC) in the Indian monsoonal rivers, and to estimate their export fluxes of
450 DIC to the north Indian Ocean, we sampled a total of 27 major and medium rivers during
451 wet period. An order of magnitude variability was found in DIC concentrations among the
452 rivers sampled ($3.4 - 73.6\text{ mg l}^{-1}$), with a lower mean concentration of $6.6 \pm 2.1\text{ mg l}^{-1}$ in rivers

453 located in the SW region of India. It is attributed to significant spatial variability in the size
454 of rivers, precipitation pattern, pollution and lithology in their catchments. The approximated
455 $\delta^{13}\text{C}$ of DIC source from the Keeling and Miller-Tans plots (-2.0 and -3.0‰ respectively)
456 and, the calculated $\delta^{13}\text{C}$ of CO_2 suggested that DIC in the Indian rivers is mainly originated
457 from chemical weathering of carbonate minerals, but largely affected by autotrophic
458 production in rivers from the southeast region of India and heterotrophic decomposition of
459 organic matter in rivers from other regions of India. Indian monsoonal rivers together export
460 $\sim 10.3 \text{ Tg yr}^{-1}$ of DIC to the north Indian Ocean, of which 7.8 Tg yr^{-1} enters in to the Bay of
461 Bengal while the Arabian Sea receives only 2.5 Tg yr^{-1} . It is mainly attributed to the volume
462 of river discharge as the former receives $\sim 378 \text{ km}^3 \text{ yr}^{-1}$ while the latter receives only 122 km^3
463 yr^{-1} from the Indian monsoonal rivers. Dense rainfall and higher soil organic carbon content
464 in the catchment of rivers from the SW region than in the catchment of the other Indian rivers
465 resulted in highest yield of DIC from the former than the latter.

466 **6. Acknowledgements**

467 We would like to thank the Director, CSIR - National Institute of Oceanography
468 (NIO), Goa, and the Scientist-In-Charge, NIO-Regional Centre, Visakhapatnam for their kind
469 support and encouragement. We also acknowledge Dr. M. Dileep Kumar, NIO, Goa for his
470 guidance and encouragement. The work is part of the Council of Scientific and Industrial
471 Research (CSIR), funded research project. This publication has NIO contribution number
472

473 **7. Data Availability**

474 The data set used in the current study can be obtained from the corresponding author by an e-
475 mail request.

476 **References**

477

478 Abril, G., Etcheber, H., Delille, B., Frankignoulle, M. and Borges A. V.: Carbonate
479 dissolution in the turbid and eutrophic Loire estuary, *Mar. Ecol. Progr. Ser.*, 259, 129-138,
480 2003.
481
482 Abongwa, P. T., and Atekwana, E. A.: Assessing the temporal evolution of dissolved
483 inorganic carbon in waters exposed to atmospheric CO₂: a laboratory approach. *J. Hydrol.*,
484 505, 250-265, 2014.
485
486 Amiotte-Suchet, P. et al.: $\delta^{13}\text{C}$ pattern of dissolved inorganic carbon in a small granitic
487 catchment: the Strengbach case study (Vosges mountains, France), *Chem. Geol.*, 159, 129–
488 145, doi:10.1016/s0009-2541(99)00037-6, 1999.
489
490 Araujo, M., Noriega, C., and Lefevre, N.: Nutrients and carbon fluxes in the estuaries of
491 major rivers flowing into the tropical Atlantic, *Front. Mar. Sci.*, 1, 1-16, 2014.
492
493 Barber, R. T., Marra, J., Bidigare, R. C., Codispoti, L. A., Halpern, D., Johnson, Z., Latasa,
494 M., Goericke, R., and Smith, S. L.: Primary productivity and its regulation in the Arabian
495 Sea during 1995, *Deep Sea Res., Part II*, 48, 1127–1172, 2001.
496
497
498 Bauer, J. E., Cai, W. J., Raymond, P. A., Bianchi, T. S., Hopkinson, C. S., and Regnier,
499 P.A.G.: The changing carbon cycle of the coastal ocean, *Nature*, 504, 61–70,
500 doi:10.1038/Nature12857, 2013.
501
502 Berner, R. A., Lasaga, A. C., Garrels, R. M.: The carbonate–silicate geochemical cycle and
503 its effect on atmospheric carbon dioxide over the past 100 million years, *Am. J. Sci.*, 283,
504 641-683, 1983
505 Bhavya, P. S., Sanjeev Kumar, Gupta, G. V. M., Sudharma, K. V., and Sudheesh, V.: Spatio-
506 temporal variation in $\delta^{13}\text{C}_{\text{DIC}}$ of a tropical eutrophic estuary (Cochin estuary, India) and
507 adjacent Arabian Sea, *Continental Shelf Research*, 153, 75-85, doi:
508 10.1016/j.csr.2017.12.006, 2018.
509
510 Boeglin, J. L., and Probst, J. L.: Physical and chemical weathering rates and CO₂
511 consumption in a tropical lateritic environment: the upper Niger basin, *Chem. Geol.*, 148;
512 137-156, 1998.
513
514 Bouillon, S., Abril, G., Borges, A. V., Dehairs, F., Govers, G., Hughes, H. J., Merckx, R.,
515 Meysman, F. J. R., Nyunja, J., Osburn, C., and Middelburg, J. J.: Distribution, origin and
516 cycling of carbon in the Tana River (Kenya): a dry season basin-scale survey from
517 headwaters to the delta, *Biogeosciences*, 6, 2475–2493, doi:10.5194/bg-6-2475-2009, 2009.
518
519 Brunet, F. *et al.* $\delta^{13}\text{C}$ tracing of dissolved inorganic carbon sources in Patagonian rivers
(Argentina). *Hydrol. Process.*, 19, 3321–3344, doi:10.1002/hyp.5973, 2005.
520
521 Cai, W. J., Guo, X. H., Chen, C. T. A., Dai, M. H., Zhang, L. J., Zhai, W. D., Lohrenz, S. E.,
522 Yin, K. D., Harrison, P. J., and Wang, Y. C.: A comparative overview of weathering intensity
523 and HCO₃ flux in the world’s major rivers with emphasis on the Changjiang, Huanghe,
524 Zhujiang (Pearl) and Mississippi Rivers, *Cont. Shelf Res.*, 28, 1538-1549, 2008.

525 Cai, W. J.: Riverine inorganic carbon flux and rate of biological uptake in the Mississippi
526 River plume, *Geophys. Res. Lett.*, 30, 1032, 2003.

527

528 Cai, W. –J.: Estuarine and coastal ocean carbon paradox: CO₂ sinks or sites of terrestrial
529 carbon incineration? *Annu Rev Mar Sci*, 3, 123-145, 2011.

530

531 Campeau, A., Wallin, M. B., Giesler, R., Löfgren, S., Mörth, C. –M., Schiff, S.,
532 Venkiteswaran, J. J. and Bishop, K.: Multiple sources and sinks of dissolved inorganic carbon
533 across Swedish streams, refocusing the lens of stable C isotopes, *Nature, Scientific Reports*,
534 7, 9158, DOI:10.1038/s41598-017-09049-9, 2017.

535

536 Carritt, D. E. and Carpenter, J. H.: Comparison and evaluation of currently employed
537 modifications of the Winkler method for determining dissolved oxygen in seawater: A
538 NASCO report, *J. Mar. Res.*, 24, 286–318, 1966.

539

540 Catalan, N., Marce, R., Kothawala, D. N. & Tranvik, L. J. Organic carbon decomposition
541 rates controlled by water retention time across inland waters. *Nature Geoscience* 9, 501–504,
542 doi:10.1038/ngeo2720, 2016.

543

544 Central Water Commission, Integrated Hydrological Data Book, 680 pp., New Delhi, 2012.

545 Central Water Commission: Integrated Hydrological Data Book, 383 pp., New Delhi, 2006.

546 Christopher, P. B., Luetlich Jr. R. A., Powers, S. P., Peterson, C. H., and McNinch, J. E.:
547 Estimating the spatial extent of bottom-water hypoxia and habitat degradation in a shallow
548 estuary, *Mar. Ecol. Prog. Ser.*, 230, 103–112, 2002.

549

550 Cole, J. J., Prairie, Y. T., Caraco, N. F., McDowell, W. H., Tranvik, L. J., Striegl, R. G.,
551 Duarte, C. M., Kortelainen, P., Downing, J. A., Middelburg, J. J., and Melack, J.: Plumbing
552 the global carbon cycle: Integrating inland waters into the terrestrial carbon budget,
553 *Ecosystems*, 10, 171–184, 2007.

554

555 Coplen, T. B.: New guidelines for reporting stable hydrogen, carbon and oxygen isotope-ratio
556 data, *Geochim. Cosmochim. Acta*, 60, 3359–3360, 1996.

557

558 Coplen, T. B. et al.: Compilation of minimum and maximum isotope ratios of selected
559 elements in naturally occurring terrestrial materials and reagents, U.S. Department of the
560 Interior and U.S. Geological Survey, 2002.

561

562 Das, A., Krishnaswami, S. and Bhattacharya, S. K.: Carbon isotope ratio of dissolved
563 inorganic carbon (DIC) in rivers draining the Deccan Traps, India: Sources of DIC and their
564 magnitudes. *Earth Planet. Sci. Lett.*, 236, 419–429, doi:10.1016/j.epsl.2005.05.009, 2005.

565

566 Deines, P., Langmuir, D., and Harmon, R. S.: Stable carbon isotope ratios and the existence
567 of a gas phase in the evolution of carbonate ground waters, *Geochim. Cosmochim. Acta*, 38,
568 1147–1164, doi:10.1016/0016-7037(74)90010-6, 1974.

569

570 Dessert, C., Dupre, B., Francois, L. M., Schott, J., Gaillardet, J., Chakrapani, G., and Bajpai, S.:
571 Erosion of Deccan Traps determined by river geochemistry: impact on the global climate and
572 the ⁸⁷Sr/⁸⁶Sr ratio of seawater. *Earth and Planet. Sci. Lett.*, 188, 459–474, 2001.

573
574 Dhillon, G. S., and Inamdar, S.: Extreme storms and changes in particulate and dissolved
575 organic carbon in runoff: Entering uncharted waters?, *Geophys. Res. Lett.*, 40, 1322–1327,
576 doi:10.1002/grl.50306., 2013.
577
578 Deirmendjian, L., and Abril, G.: Carbon dioxide degassing at the groundwater-stream
579 atmosphere interface: isotopic equilibration and hydrological mass balance in a sandy
580 watershed, *J. Hydrol.*, 2018, doi: <https://doi.org/10.1016/j.jhydrol.2018.01.003>
581
582 Findlay, S.: Stream microbial ecology, *J. North Am. Benthol. Soc.*, 29, 170–181,
583 doi:10.1899/09-023.1, 2010.
584
585 Finlay, J. C. and Kendall, C.: Stable isotope tracing of temporal and spatial variability in
586 organic matter sources to freshwater ecosystems, In: *Stable Isotopes in Ecology and*
587 *Environmental Science*, 2nd edn., edited by: Michener, R. H. and Lajtha, K., Blackwell
588 Publishing, Malden, USA, 283–333, 2007.
589
590 Finlay, J. C.: Controls of stream water dissolved inorganic carbon dynamics in a forested
591 watershed, *Biogeochem.*, 62, 231–252, 2003.
592
593 Finlay, J. C.: Patterns and controls of lotic algal stable carbon isotope ratios, *Limnol.*
594 *Oceanogr.*, 49, 850–861, 2004.
595
596 Gaillardet, J., Dupre, B., Louvat, P., and Allegre, C. J.: Global silicate weathering and CO₂
597 consumption rates deduced from the chemistry of large rivers. *Chem. Geol.* 159, 3–30, 1999.
598
599 Gauns, M., Madhupratap, M., Ramaiah, N., Jyothibabu, R., Fernandes, V., Paul, J. T., and
600 Kumar, S. P.: Comparative accounts of biological productivity characteristics and estimates
601 of carbon fluxes in the Arabian Sea and the Bay of Bengal, *Deep Sea Res., Part II*, 52, 2003–
602 2017, 2005.
603
604 Garcia, E. H., and Gordon, L. I.: Oxygen solubility in seawater better fitting equations,
605 *Limnol. Oceanogr.*, 37, 1307–1312, doi:10.4319/lo.1992.37.6.1307, 1992.
606
607 Giesler, R. *et al.* Spatiotemporal variations of pCO₂ and δ¹³C-DIC in subarctic streams in
608 northern Sweden. *Global Biogeochemical Cycles* 27, 176–186, doi:10.1002/gbc.20024, 2013.
609
610 Gupta, G.V.M., Sarma, V.V.S.S., Robin, R.S., Raman, A.V., Jai Kumar, M., Rakesh, M. and
611 Subramanian, B. R.: Influence of net ecosystem metabolism in transferring riverine organic
612 carbon to atmospheric CO₂ in a tropical coastal lagoon (Chilka Lake, India).
613 *Biogeochemistry*, 87, 265–285, doi:10.1007/s10533-008-9183-x, 2008.
614
615 Gupta, G. V. M., Thottathil, S. D., Balachandran, K. K., Madhu, N. V., Madeswaran, P., and
616 Nair, S.: CO₂ supersaturation and net heterotrophy in a tropical estuary (Cochin, India):
617 influence of anthropogenic effect, *Ecosystems*, 12, 1145–1157, doi:10.1007/s10021-009-
618 9280-2, 2009.
619
620 Gupta, H., Chakrapani, G. J., Selvaraj, K., and Kao, S.-J.: The fluvial geochemistry,
621 contributions of silicate, carbonate and saline–alkaline components to chemical weathering

622 flux and controlling parameters: Narmada River (Deccan Traps), India, *Geochim. Cosmochi.*
623 *Acta*, 75, 800-824, 2011.

624

625 Gurumurthy G. P., Balakrishna K., Riotte J., Braun J.-J., Audry S., Shankar H. N. U. and
626 Manjunatha B. R.: Controls on intense silicate weathering in a tropical river, southwestern
627 India, *Chem. Geol.*, 300–301, 61–69, 2012.

628

629 Hotchkiss, E. R. *et al.* Sources of and processes controlling CO₂ emissions change with the
630 size of streams and rivers, *Nature Geoscience* 8, doi:10.1038/Ngeo2507, 2015.

631

632 Huang, T-H., Fu, Y-H., Pan, P-Y., and Arthur, C.T.: Fluvial carbon fluxes in tropical rivers,
633 *Current Opinion in Environmental Sustainability*, 4, 162–169, 2012.

634

635 Ishikawa, N.F., Tayasu, I., Yamane, M., Yokoyama, Y., Sakai, S., and Ohkouchi, N.: Sources
636 of dissolved inorganic carbon in two small streams with different bedrock geology; Insights
637 from carbon isotopes. *Radiocarbon*, 57, 439–448, 2015.

638

639 Jarvie, H.P., King, S.M., and Neal, C.: Inorganic carbon dominates total dissolved carbon
640 concentrations and fluxes in British rivers: Application of the THINCARB model –
641 Thermodynamic modeling of inorganic carbon in freshwaters, *Sci. Tot. Environ.*, 575, 496-
642 512, 2017.

643

644 Joesoef, A., Kirchman, D. L., Sommerfield, C.K., and Cai, W-J.: Seasonal variability of the
645 inorganic carbon system in a large coastal plain estuary. *Biogeosciences*, 14, 4949-4963,
646 2017

647

648 Keeling, C. D.: The concentration and isotopic abundances of atmospheric carbon dioxide in
649 rural areas. *Geochimica et Cosmochimica Acta* **13**, 322–334, doi:10.1016/0016-
650 7037(58)90033-4 (1958).

651

652 Kishwan, J., Pandey, R., and Dhadwal, V. K.: India’s forest and tree cover: Contribution as a
653 carbon sink, Tech. Pap. 130, ICFRE BL-23, 2009.

654

655 Krishna, M. S., Prasad, V. R., Sarma, V. V. S. S., Reddy, N. P. C., Hemalatha, K. P. J., and
656 Rao Y. V.: Fluxes of dissolved organic carbon and nitrogen to the northern Indian Ocean from
657 the Indian monsoonal rivers, *J. Geophys. Res. Biogeosci.*, 120, 2067–2080, 2015.

658

659 Kumar, R., Singh, R. D., and Sharma, K. D.: Water resources of India, *Curr. Sci.*, 89, 794–
660 811, 2005.

661

662 Land, L. S.: The isotopic and trace element geochemistry of dolomite: the state of the art.
663 *Concepts and Models of Dolomitization*, 63, 485, doi:10.2110/pec.80.28.0087, 1980.

664

665 Lerman, A., Wu, L. L., and Mackenzie, F. T.: CO₂ and H₂SO₄ consumption in weathering
666 and material transport to the ocean, and their role in the global carbon balance, *Mar. Chem.*,
667 106, 326-350, 2007.

668

669 Löfgren, S., Froberg, M., Yu, J., Nisell, J. & Ranneby, B.: Water chemistry in 179 randomly
670 selected Swedish headwater streams related to forest production, clear-felling and climate.
671 *Environ Monit Assess* 186, 8907–8928, doi:[10.1007/s10661-014-4054-5](https://doi.org/10.1007/s10661-014-4054-5), 2014.

672

673 Ludwig, W., Amiotte-Suchet, P., Munhoven, G., and Probst, J. L.: Atmospheric CO₂
674 consumption by continental erosion: present-day controls and implications for the last glacial
675 maximum. *Global Planet Change*, 17, 107-120, 1998.

676

677 Mackenzie, F. T., Lerman, A., and Andersson, A.J.: Past and present of sediment and carbon
678 biogeochemical cycling models. *Biogeosciences* 1, 11 -32, 2004.

679

680 Madhupratap, M., Prasanna Kumar, S., Bhattathiri, P. M. A., Kumar, M. D., Raghukumar, S.,
681 Nair, K. K. C., and Ramaiah, N.: Mechanism of the biological response to winter cooling in
682 the northeastern Arabian Sea, *Nature*, 384, 549–552, 1996.

683

684 Maher, D. T., Cowley, K., Santos, I. R., Macklin, P., and Eyre, B. D.: Methane and carbon
685 dioxide dynamics in a subtropical estuary over a diel cycle: Insights from automated *in situ*
686 radioactive and stable isotope measurements, *Mar. Chem.*, 168, 69–79,
687 doi:[10.1016/j.marchem.2014.10.017](https://doi.org/10.1016/j.marchem.2014.10.017), 2015.

688

689 Maher, D. T., Santos, I. R., Golsby-Smith, L., Gleeson, J., and Eyre, B. D.: Groundwater-
690 derived dissolved inorganic and organic carbon exports from a mangrove tidal creek: The
691 missing mangrove carbon sink?, *Limnol. Oceanogr.*, 58, 475-488,
692 doi:[10.4319/lo.2013.58.2.0475](https://doi.org/10.4319/lo.2013.58.2.0475), 2013.

693

694 Mayorga, E. *et al.* Young organic matter as a source of carbon dioxide outgassing from
695 Amazonian rivers. *Nature* **436**, 538–541, doi:[10.1038/nature03880](https://doi.org/10.1038/nature03880), 2005.

696

697 McConnaughey, T. A., LaBaugh, J. W., Rosenberry, D. O., Striegl, R. G., Reddy, M. M.,
698 Schuster, P. F., and Carter, V.: Carbon budget for a groundwater-fed lake: calcification
699 supports summer photosynthesis, *Limnol. Oceanogr.*, 39, 1319–1332, 1994.

700

701 Meybeck, M., and Ragu, A.: GEMS/water contribution to the Global Register of River Inputs
702 (GLORI), Provisional Final Rep., 245 pp., UNEP/WHO/UNESCO, Geneva, Switzerland,
703 1995.

704

705 Meybeck, M., and Ragu, A.: River discharges to the oceans. An assessment of suspended
706 solids, major ions, and nutrients, *Environ. Inf. and Assess. Rep.*, 250, 1996.

707

708 Meybeck, M., and Vorosmarty, C. J.: Global transfer of carbon by rivers, *Global Change*
709 *News Lett*, 37, 41974, 1999.

710

711 Meybeck, M.: Global chemical weathering of surficial rocks estimated from river dissolved
712 loads, *Am. J. Sci.*, 287, 401–428, 1987.

713

714

715 Meybeck, M.: Riverine Transport of atmospheric carbon-sources, global typology and
716 budget. *Water Air Soil Pollut.*, 70, 443-463, 1993.

717

718 Miller, J. B. & Tans, P. P.: Calculating isotopic fractionation from atmospheric measurements
719 at various scales. *Tellus B* 55, 207–214, doi:[10.1034/j.1600-0889.2003.00020.x](https://doi.org/10.1034/j.1600-0889.2003.00020.x) (2003).
720

721 Mukhopadhyay, S. K., Biswas, H., De, T. K., Sen, S., and Jana, T. K.: Seasonal effects on the
722 air–water carbon dioxide exchange in the Hooghly estuary, NE coast of Bay of Bengal, India.
723 *J Environ Monit.*, 4, 549-552, 2002.
724

725 Muraleedharan, P. M., and Prasanna Kumar, S.: Arabian Sea upwelling—A comparison
726 between coastal and open ocean regions, *Curr. Sci.*, 71, 842–846, 1996.
727

728 O’Leary, M. H.: Carbon Isotopes in Photosynthesis, *BioScience*, 38, 328–336, doi:
729 [10.2307/1310735](https://doi.org/10.2307/1310735), 1988.
730

731 Opsahl, S. P. and Zepp, R. G.: Photochemically-induced alteration of stable carbon isotope
732 ratios ($\delta^{13}\text{C}$) in terrigenous dissolved organic carbon, *Geophys. Res. Lett.*, 28, 2417–2420,
733 doi:[10.1029/2000gl012686](https://doi.org/10.1029/2000gl012686), 2001.
734

735 Parker, S. R., Poulson, S. R., Gammons, C. H., and DeGrandpre, M. D.: Biogeochemical
736 controls on diel cycling of stable isotopes of dissolved O_2 and dissolved inorganic carbon in
737 the Big Hole River, Montana, *Environ. Sci. Tech.*, 39, 7134–7140, doi:[10.1021/es0505595](https://doi.org/10.1021/es0505595),
738 2005.
739

740 Parker, S. R., Poulson, S. R., Smith, M. G., Weyer, C. L., and Bates, K. M.: Temporal
741 variability in the concentration and stable carbon isotope composition of dissolved inorganic
742 and organic carbon in two Montana, USA Rivers, *Aquat Geochem.*, 16, 61–84,
743 doi:[10.1007/s10498-009-9068-1](https://doi.org/10.1007/s10498-009-9068-1), 2010.
744

745 Pataki, D. E. *et al.* The application and interpretation of Keeling plots in terrestrial carbon
746 cycle research. *Global Biogeochemical Cycles* 17, 1022, doi:[10.1029/2001GB001850](https://doi.org/10.1029/2001GB001850) (2003).
747

748 Pattanaik, J. K., Balakrishnan, S., Bhutani, R. and Singh, P.: Estimation of weathering rates
749 and CO_2 drawdown based on solute load: Significance of granulites and gneisses dominated
750 weathering in the Kaveri River basin, Southern India, *Geochim. Cosmochim. Acta*, 121, 611-
751 636, 2013.
752

753 Pattanaik, S., Sahoo, R. .K, Satapathy, D. R., Panda, C. R., Choudhury, S. B. et al.: Intra-
754 annual Variability of CO_2 Flux in the Mahanadi Estuary- A Tropical Estuarine System, India.
755 *Ann Mar Sci.*, 1, 005-012, 2017.
756

757 Polsenaere, P., and Abril, G.: Modelling CO_2 degassing from small acidic rivers using water
758 pCO_2 , DIC and $\delta^{13}\text{C}$ -DIC data. *Geochim. Cosmochim. Acta* 91, 220–239, 2012
759 doi:[10.1016/j.gca.2012.05.030](https://doi.org/10.1016/j.gca.2012.05.030)

760 Prasanna Kumar, S., Muraleedharan, P. M., Prasad, T. G., Gauns, M., Ramaiah, N., de Souza,
761 S. N., Sardesai, S., and Madhupratap, M.: Why is the Bay of Bengal less productive during
762 summer monsoon compared to the Arabian Sea?, *Geophys. Res. Lett.*, 29, 2235,
763 doi:[10.1029/2002GL016013](https://doi.org/10.1029/2002GL016013), 2002.
764

765 Prasanna Kumar, S., Nuncio, M., Narvekar, J., Kumar, A., Sardesai, S., DeSousa, S. N.,
766 Gauns, M., Ramaiah, N., and Madhupratap, M.: Are eddies nature's trigger to enhance

767 biological productivity in the Bay of Bengal? *Geophys. Res. Lett.* 31, 5.
768 doi:10.1029/2003G1019274, 2004.
769

770 Quay, P. D. *et al.* Carbon cycling in the Amazon River: Implications from the ^{13}C
771 compositions of particles and solutes. *Limnology and Oceanography* 37, 857–871,
772 doi:10.4319/lo.1992.37.4.0857, 1992.
773

774 Raymond, P. A., and Cole, J. J.: Increase in the export of alkalinity from North America's
775 largest river, *Science*, 301, 88–91, doi:10.1126/science.1083788, 2003.
776

777 Raymond, P. A., Oh, N. H., Turner, R. E., and Broussard, W.: Anthropogenically enhanced
778 fluxes of water and carbon from the Mississippi River, *Nature*, 451, 449–452,
779 doi:10.1038/Nature06505, 2008.
780

781 Raymond, P.A., and Bauer, J.: Atmospheric CO_2 evasion, dissolved inorganic carbon
782 production, and net heterotrophy in the York River estuary, *Limnol.Oceanogr.*, 45, 1707-
783 1717, 2000.
784

785 Regnier, P., et al.: Anthropogenic perturbation of the carbon fluxes from land to ocean, *Nat.*
786 *Geosci.*, 6, 597–607, doi:10.1038/ngeo1830, 2013.
787

788 Ren, W., Tian, H., Tao, B., Yang, J., Pan, S., Cai, W.-J., Lohrenz, S. E., He, R., and
789 Hopkinson, C. S.: Large increase in dissolved inorganic carbon flux from the Mississippi
790 River to Gulf of Mexico due to climatic and anthropogenic changes over the 21st century, *J.*
791 *Geophys. Res. Biogeosci.*, 120, 724–736, doi:10.1002/2014JG002761, 2015.
792

793 Rengarajan, R., and Sarma, V. V. S. S.: Submarine groundwater discharge and nutrient
794 addition to the coastal zone of the Godavari estuary, *Mar. Chem.*, 172, 57-69, 2015.
795 Richey, J.E. et al: Outgassing from Amazonian rivers and wetlands as a large tropical source
796 of atmospheric CO_2 , *Nature* 416, 617-620, 2002

797 Samanta, S., Dalai, T. K., Pattanai K. J. K., Rai, S. K., and Mazumdar, A.: Dissolved
798 inorganic carbon (DIC) and its $\delta^{13}\text{C}$ in the Ganga (Hooghly) River estuary, India: Evidence
799 of DIC generation via organic carbon degradation and carbonate dissolution.
800 *Geochim.Cosmochim.Acta*, 165, 226–248, 2015.
801

802 Sarma, V. V. S. S., et al.: Emission of carbon dioxide from the Indian monsoonal estuaries,
803 *Geophys. Res. Lett.*, 39, L03602, doi:10.1029/2011GL050709, 2012.
804

805 Sarma, V. V. S. S., et al.: High CO_2 emissions from the tropical Godavari estuary (India)
806 associated with monsoon river discharges, *Geophys. Res. Lett.*, 38, L08601,
807 doi:10.1029/2011GL046928, 2011.
808

809 Sarma, V. V. S. S., Kumar, M. D., and Manerikar, M.: Emission of carbon dioxide from a
810 tropical estuarine system, Goa, India, *Geophys. Res. Lett.*, 28, 1239–1242,
811 doi:10.1029/2000GL006114, 2001.
812

813 Sarma, V. V. S. S., Krishna, M. S., Prasad, V. R., Kumar, B. S. K., Naidu, S. A., Rao, G. D.,
814 Viswanadham, R., Sridevi, T., Kumar, P. P., and Reddy, N. P. C.: Distribution and sources of
815 particulate organic matter in the Indian monsoonal estuaries during monsoon, *J. Geophys.*
816 *Res. Biogeosci.*, 119, doi:10.1002/2014JG002721, 2014.

817
818 Shetye, S. R., Gouveia, A. D., Shenoi, S. S. C.: Circulation and water masses of the Arabian
819 Sea, *Proc. Indian Acad. Sci. Earth Planet. Sci.*, 103, 107–123, 1994.

820
821 Shin, W. J., Chung, G. S., Lee, D., and Lee, K. S.: Dissolved inorganic carbon export from
822 carbonate and silicate catchments estimated from carbonate chemistry and $\delta^{13}\text{C}_{\text{DIC}}$. *Hydrol.*
823 *Earth Syst. Sci.*, 15, 2551 – 2560, 2011.

824
825 Singh, S.K., Sarin, M.M., and France-Lanord, C.: Chemical erosion in the eastern Himalaya:
826 Major ion composition of the Brahmaputra and ^{13}C of dissolved inorganic carbon. *Geochim.*
827 *Cosmochim. Acta*, 69, 3573-3588, 2005.

828
829 Smith S. L.: Understanding the Arabian Sea: reflections on the 1994–1996 Arabian Sea
830 expedition, *Deep Sea Res. Part II* 48, 1385–1402, 2001.

831
832 Solomon, D. K., and Cerling, T. E.: The annual carbon dioxide cycle in a montane soil:
833 observations, modeling and implications for weathering, *Water Resources Res.*, 23, 2257-
834 2265, 1987.

835
836 Soman, M. K., and Kumar, K. K.: Some aspects of daily rainfall distribution over India
837 during the southwest monsoon season, *Int. J. Clim.*, 19, 299–311, 1990.

838
839 Sreenivas, K., Dadhwal, V. K., Suresh, K., Sri Harsha, G., Tarik, M., Sujatha, G, Suresh, J.
840 R., G., Fyze, M., and Ravisankar, T.: Digital mapping of soil organic and inorganic carbon
841 status in Indi, *Geoderm.*, 269. 160-173, 10.1016/j.geoderma.2016.02.002, 2016.

842
843 Sridevi, B., Sarma, V.V.S.S., Murty, T.V.R., Sadhuram, Y., Reddy, N.P.C., Vijayakumar, K.,
844 Raju, N.S.N., Jawahar Kumar, Ch., Raju, Y.S.N., Luis, R., Kumar, M.D., Prasad, K.V.S.R. :
845 Variability in stratification and flushing times of the Gautami–Godavari estuary, India, *J.*
846 *Earth. Sys., Sci.*, 124, 993-1003, 2015.

847
848 Subramanian, V.: Sediment load of Indian rivers, *Curr. Sci.*, 64, 928–930, 1993.

849
850 Suzuki, R., and Ishimaru, T.: An improved method for the determination of phytoplankton
851 chlorophyll using N,N-dimethyl formamide, *J. Oceanogr.*, 46, 190–194, 1990.

852
853 Tamoo, F., Borges, A. V., Meysman, F. J. R., Meersche, K. V. D., Dehairs, F., Merckx, R.
854 et al.: Dynamics of dissolved inorganic carbon and aquatic metabolism in the
855 Tana River Basin, Kenya, *Biogeosciences Discuss.*, 10, 5175–5221, 2013.

856
857 Tamse, S., Ogrinc, N., Walter, L.M, Turk, D., and Faganeli, J.: River Sources of Dissolved
858 Inorganic Carbon in the Gulf of Trieste (N Adriatic): Stable Carbon Isotope Evidence,
859 *Estuaries and Coasts*, DOI 10.1007/s12237-014-9812-7, 2014.

860

- 861 Tank, J. L., Rosi-Marshall, E. J., Griffiths, N. A., Entekin, S. A., and Stephen, M. L.: A
862 review of allochthonous organic matter dynamics and metabolism in streams, *J. North Am.*
863 *Benthol. Soc.*, 29, 118–146, doi:10.1899/08-170.1, 2010.
- 864
- 865 Vähätalo, A. V., and Wetzel, R. G.: Long-term photochemical and microbial decomposition
866 of wetland-derived dissolved organic matter with alteration of $^{13}\text{C}:^{12}\text{C}$ mass ratio, *Limnol.*
867 *Oceanogr.*, 53, 1387–1392, doi:10.4319/lo.2008.53.4.1387, 2008.
- 868
- 869 Varkey, M. J., Murty, V. S. N., and Suryanarayana, A.: Physical oceanography of the Bay of
870 Bengal and Andaman Sea, *Oceanogr. Mar. Biol.*, 34, 1–70, 1996.
- 871 Venkiteswaran, J.J., Schiff, S.L., and Wallin, M.B.: Large Carbon Dioxide Fluxes from
872 Headwater Boreal and Sub-Boreal Streams. *PLoS ONE* 9, e101756, 2014.
- 873
- 874 Viers, J., Oliva, P., Dandurand, J. L., Dupré, B., Gaillardet, J., Heinrich, D. H., and Karl, K.
875 T.: Chemical weathering rates, CO_2 consumption, and control parameters deduced from the
876 chemical composition of Rivers, *Treatise on Geochemistry* Pergamon, Oxford, 2007.
- 877
- 878 Vijith, V., Sundar, D., and Shetye, S. R.: Time-dependence of salinity in monsoonal
879 estuaries, *Estuar. Coast. Shelf Sci.*, 85, 601–608, doi:10.1016/j.ecss.2009.10.003, 2009.
- 880
- 881 Waldron, S., Hall, A. J., and Fallick, A. E.: Enigmatic stable isotope dynamics of deep peat
882 methane, *Glob. Biogeochem. Cy.*, 13, 93–100, doi:10.1029/1998gb900002, 1999.
- 883
- 884 Waldron, S., Scott, E. M., and Soulsby, C.: Stable isotope analysis reveals lower-order river
885 dissolved inorganic carbon pools are highly dynamic, *Environ. Sci. Technol.*, 41, 6156–6162,
886 doi:10.1021/es0706089, 2007.
- 887
- 888 Wang, Z. A., Bienvenu, D.J., Mann, P.J., Hoering, K.A. Poulsen, J.R., Spencer, R.G.M., and
889 Holmes, R.M.: Inorganic carbon speciation and fluxes in the Congo River, *Geophys. Res.*
890 *Lett.*, 40, 511–516, 2013.
- 891
- 892 Williamson, C. E., Zagarese, H. E., Schulze, P. C., Hargreaves, B. R., and Seva, J.: The
893 impact of short-term exposure to UV-B radiation on zooplankton communities in north
894 temperate lakes, *J. Plankton Res.*, 16, 205–218, doi:10.1093/plankt/16.3.205, 1994.
- 895
- 896 Zeng, F- W., Masiello C. A., and Hockaday, W. C.: Controls on the origin and cycling of
897 riverine dissolved inorganic carbon in the Brazos River, Texas, *Biogeochemistry*, 104, 275–
898 291, doi:10.1007/s10533-010-9501-y, 2011.
- 899
- 900 Zou, J.: Sources and Dynamics of Inorganic Carbon within the Upper Reaches of the Xi
901 River Basin, Southwest China, *PLoS One*, 11, e0160964. doi:10.1371/journal.pone.0160964,
902 2016.
- 903
- 904
- 905

906 **Figure captions**

907

908 **Figure 1:** Map showing the study region. Rivers sampled in this study were indicated by
909 solid black line. Distribution of soils in catchments of the Indian monsoonal rivers sampled

910 was also shown. Rivers draining the four regions, i.e., northwest (NW), southwest (SW),
911 southeast (SE) and northeast (NE) were shown by solid black arrows.

912

913 **Figure 2:** Schematic diagram showing the typical range of $\delta^{13}\text{C}$ of different sources of
914 dissolved inorganic carbon (DIC) in rivers. Various major processes influencing the $\delta^{13}\text{C}$ of
915 DIC ($\delta^{13}\text{C}_{\text{DIC}}$) within the rivers were also shown. Hollow black arrows (\Leftarrow and \Rightarrow) indicates
916 the direction of change in $\delta^{13}\text{C}_{\text{DIC}}$ due to the influences different in-stream process mentioned
917 against arrows.

918

919 **Figure 3:** Spatial variability in the concentration (mg l^{-1} ; 3a), export flux (Tg yr^{-1} ; 3b) and
920 yield ($\text{g m}^{-2} \text{yr}^{-1}$; 3c) of dissolved inorganic carbon (DIC) and its stable isotopes ($\delta^{13}\text{C}_{\text{DIC}}$, 3d)
921 in the Indian monsoonal rivers studied. Rivers geographically located in the northwest (NW),
922 southwest (SW), southeast (SE) and northeast (NE) regions of India were also shown. Rivers
923 draining into the Bay of Bengal (east-flowing rivers) were shown by gray shade while rivers
924 draining into the Arabian Sea (west-flowing) were shown by no shade.

925

926 **Figure 4:** (a) Exponential decrease and (b) linear increase of dissolved inorganic carbon
927 (DIC) concentrations with increasing the rainfall over the catchment and length of the river
928 respectively. (c) Inverse and (d) linear relationships of chlorophyll-a (Chl-a) with
929 concentrations and $\delta^{13}\text{C}$ of DIC respectively. Significant linear relationships of $\delta^{13}\text{C}$ of DIC
930 with (e) dissolved oxygen (DO) saturation and (f) dissolved organic carbon (DOC)
931 concentration. Linear relationships observed between (g) DIC concentrations and population
932 density in the catchment and (h) total alkalinity and $\delta^{13}\text{C}$ of DIC in the Indian monsoonal
933 rivers during the study period. Ovals with dashed line indicate the outliers which were not
934 included in the regression equations. Rivers of the northwest region of India showed linear
935 relationships as shown by the other Indian rivers but with a different slope (Fig. f-h)

936

937 **Figure 5:** Least square linear regression models of (a) $\delta^{13}\text{C}_{\text{DIC}}$ as a function of $1/\text{DIC}$
938 (Keeling plot) and (b) $\delta^{13}\text{C}_{\text{DIC}} \times \text{DIC}$ as a function of DIC concentrations (Miller-Tans plot) in
939 the Indian monsoonal rivers. (c) Linear relationship between calculated $\delta^{13}\text{C}$ of CO_2 and the
940 measured $\delta^{13}\text{C}_{\text{DIC}}$ and (d) Miller-Tans linear regression model of $\delta^{13}\text{C}-\text{CO}_2 \times \text{CO}_2$ as a
941 function of CO_2 concentration in the Indian monsoonal rivers.

942

943 **Figure 6:** Significant relationships of dissolved inorganic carbon (DIC) yield with (a) river
944 discharge in medium estuaries, (b) catchment areas of the medium rivers, (c) catchment areas
945 of the major rivers, (d) rainfall over the catchment of all the rivers sampled and (e) soil
946 organic carbon (OC) content in catchments of the Indian monsoonal rivers studied. Since the
947 data on soil OC is not available for each watershed (e) was plotted using the available soil
948 OC data on regional scale (NW, SW, SE and NE regions of India), Hence, it contains only
949 four points.

950

951

952

953

954

955

956

957

958 **Table captions**

959

960 **Table 1:** Catchment area, discharge, length and elevation of each river and, annual mean
961 rainfall, number of dams and population density in each watershed of the Indian monsoonal
962 rivers sampled. Concentrations, export fluxes and yields of dissolved inorganic carbon (DIC)
963 and its stable isotopes ($\delta^{13}\text{C}_{\text{DIC}}$) of Indian rivers were given. Measured pH and calculated
964 $\delta^{13}\text{C}$ of CO_2 from isotopic fractionation factors across DIC speciation were also provided.
965 Rivers located in the northern region (north of 16°N) of India were shown by the shaded
966 (grey) area. Of these rivers, Mahisagar, Sabarmati, Tapti and Narmada are located in the
967 northwestern (NW) whereas, rivers from Godavari to Hyadri are located in the northeastern
968 (NE) region of India.

969

970

971

972

973

974

River name	Catchment area (x10 ³ km ²)	Annual Discharge (km ³)	Length (km)	Population (No. km ⁻²)	No. of major Dams	Elevation (m)	Rain-fall (mm)	pH	DIC Conc. (mg l ⁻¹)	DIC export flux (Tg yr ⁻¹)	DIC yield (g m ⁻² yr ⁻¹)	δ ¹³ C _{DIC} (‰)	Cal. δ ¹³ C-CO ₂ (‰)
West flowing rivers (Arabian Sea)													
MAHISAGAR	34.8	11.0	580	507	138	500	785	7.3	22.8	0.3	7.2	-12.4	-21.5
SABARMATI	21.7	3.8	371	1702	62	1173	787	7.2	24.6	0.1	4.3	-13.0	-
TAPTI	65	14.9	724	208	375	752	888	7.1	35.6	0.5	8.2	-7.9	-16.4
NARMADA	99	45.6	1312	184	281	1317	1120	7.5	30.6	1.4	14.1	-11.0	-
ZUARI	1	3.2	34	92	3	-	3500	7.0	4.8	0.0	4.4	-5.1	-13.2
MANDOVI	3.6	3.3	81	62	2	600	3500	6.5	4.5	0.0	14.5	-7.4	-13.6
KHALI	4.2	4.8	184	111	6	600	3200	7.2	5.7	0.0	6.5	-7.0	-15.5
SHARAVATHI	3.6	4.5	128	109	3	700	4000	6.5	8.4	0.0	10.6	-6.8	-13.1
NETRAVATHI	3.2	11.1	103	103	-	1000	3923	6.3	5.1	0.1	17.8	-7.1	-12.4
BHARATHAPUZHA	6.2	5.1	209	-	13	1964	2500	6.0	3.4	0.0	2.8	-7.9	-11.6
CHALAKUDY	1.7	1.9	144	-	6	1250	3600	6.3	4.8	0.0	5.4	-5.1	-10.3
East flowing rivers (Bay of Bengal)													
VAIGAI	7	1.1	258	499	2	1200	850	-	26.0	0.0	4.2	-7.9	-
AMBALAYAAR	-	0.9	-	-	-	-	-	8.6	32.2	0.0	-	-	-
CAUVERY	88	21.3	800	393	122	1341	1075	7.5	40.5	0.9	9.8	-2.9	-11.8
VELLAR	8.6	0.9	210	457	3	900	980	7.4	73.6	0.1	7.7	-2.4	-11.1
PONNAIYAR	16	1.6	396	291	4	900	969	7.4	43.4	0.1	4.3	-1.4	-10.3
PENNA	55	6.3	597	186	61	1439	510	8.3	37.1	0.2	4.3	-2.6	-11.9
KRISHNA	259	69.8	1300	260	736	1903	784	8	33.5	2.3	9.0	-3.9	-
GODAVARI	313	110.5	1465	193	978	1067	1300	-	13.1	1.5	4.6	-5.6	-9.6
NAGAVALI	9.4	2.0	256	150	4	1300	1000	-	15.5	0.0	3.3	-	-13.1
VAMSADHARA	11.0	3.5	254	130	3	370	1400	8.2	27.2	0.1	8.6	-3.0	-12.4
RUSIKULYA	9.0	1.9	175	360	13	1000	1000	-	19.8	0.0	4.2	-	-
MAHANADI	141.6	66.9	858	282	280	890	1406	6.9	13.3	0.9	6.3	-5.4	-13.2
BAITARANI	14.2	28.5	414	324	8	900	1450	6.0	10.3	0.3	20.7	-6.5	-10.2
SUBARNALEKHA	29.2	12.4	395	338	12	600	1800	8.0	13.6	0.2	5.8	-2.9	-12.0
HYADRI	10.2	50.5		191				7.1	24.1	1.2	-	-5.8	-14.0

Table 1

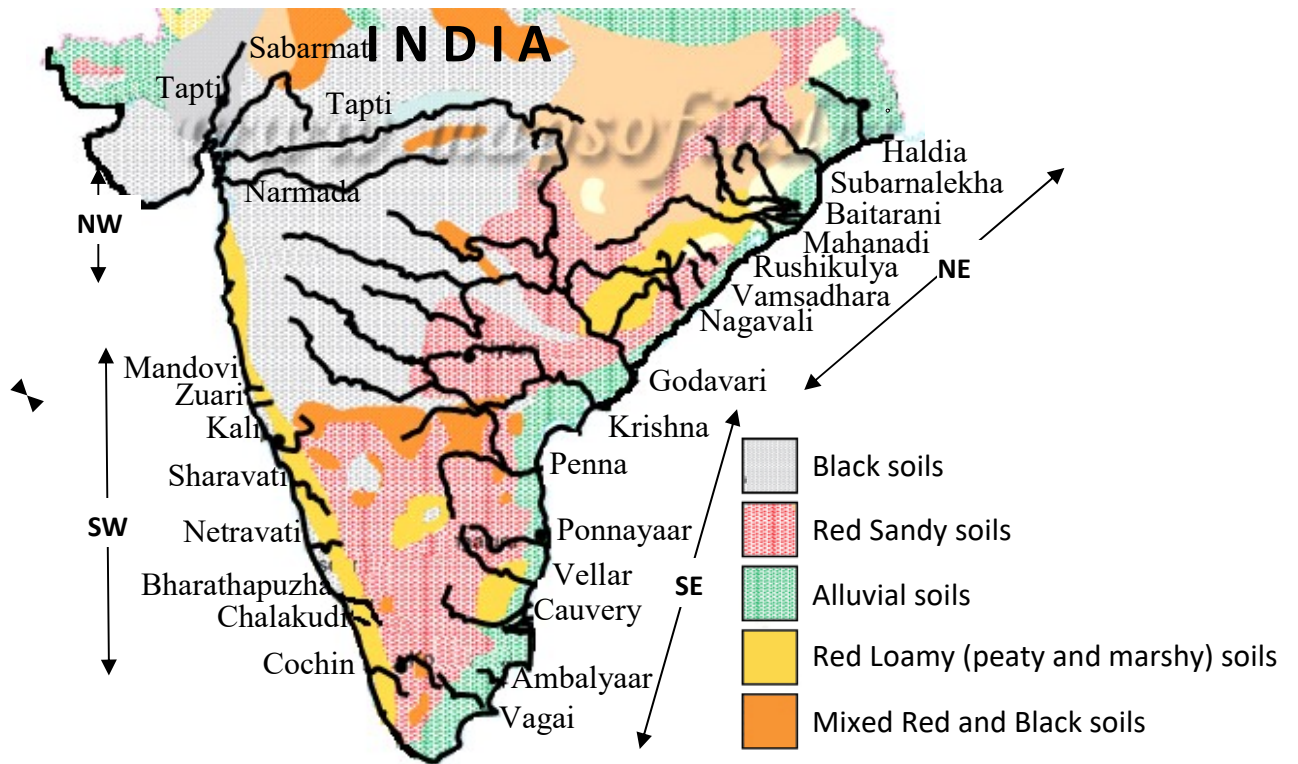


Fig. 1

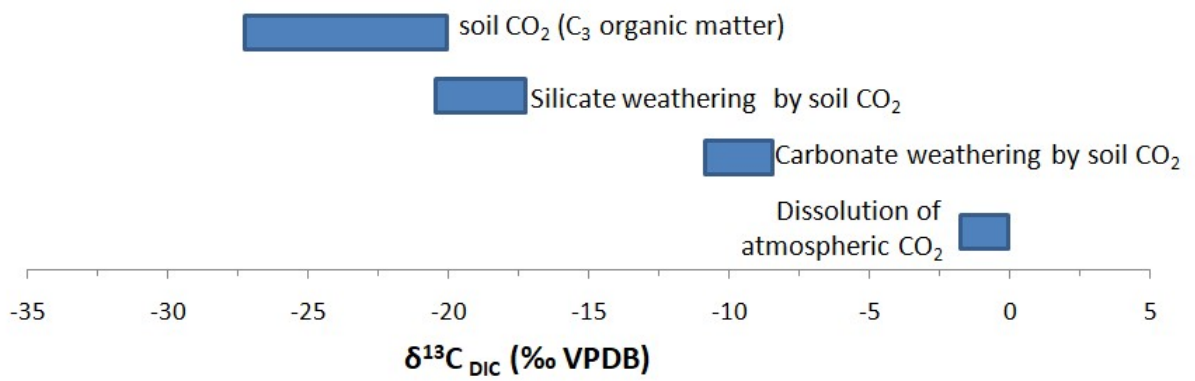
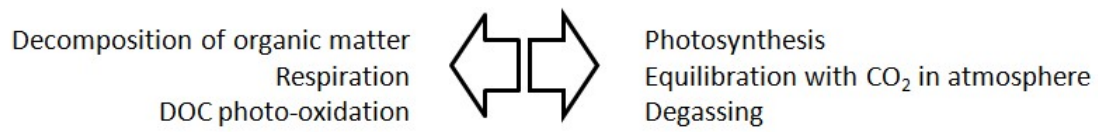


Fig. 2

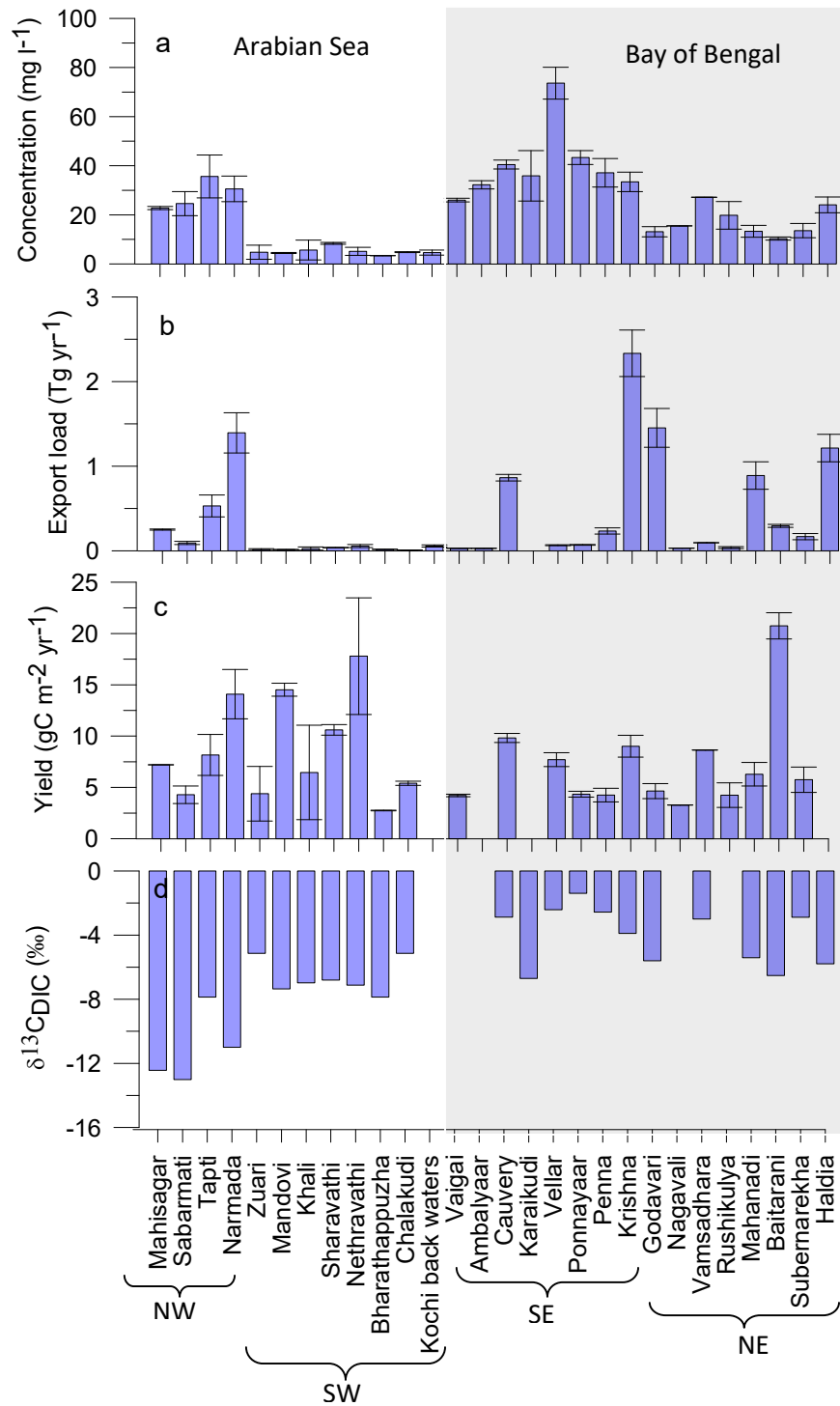


Fig. 3

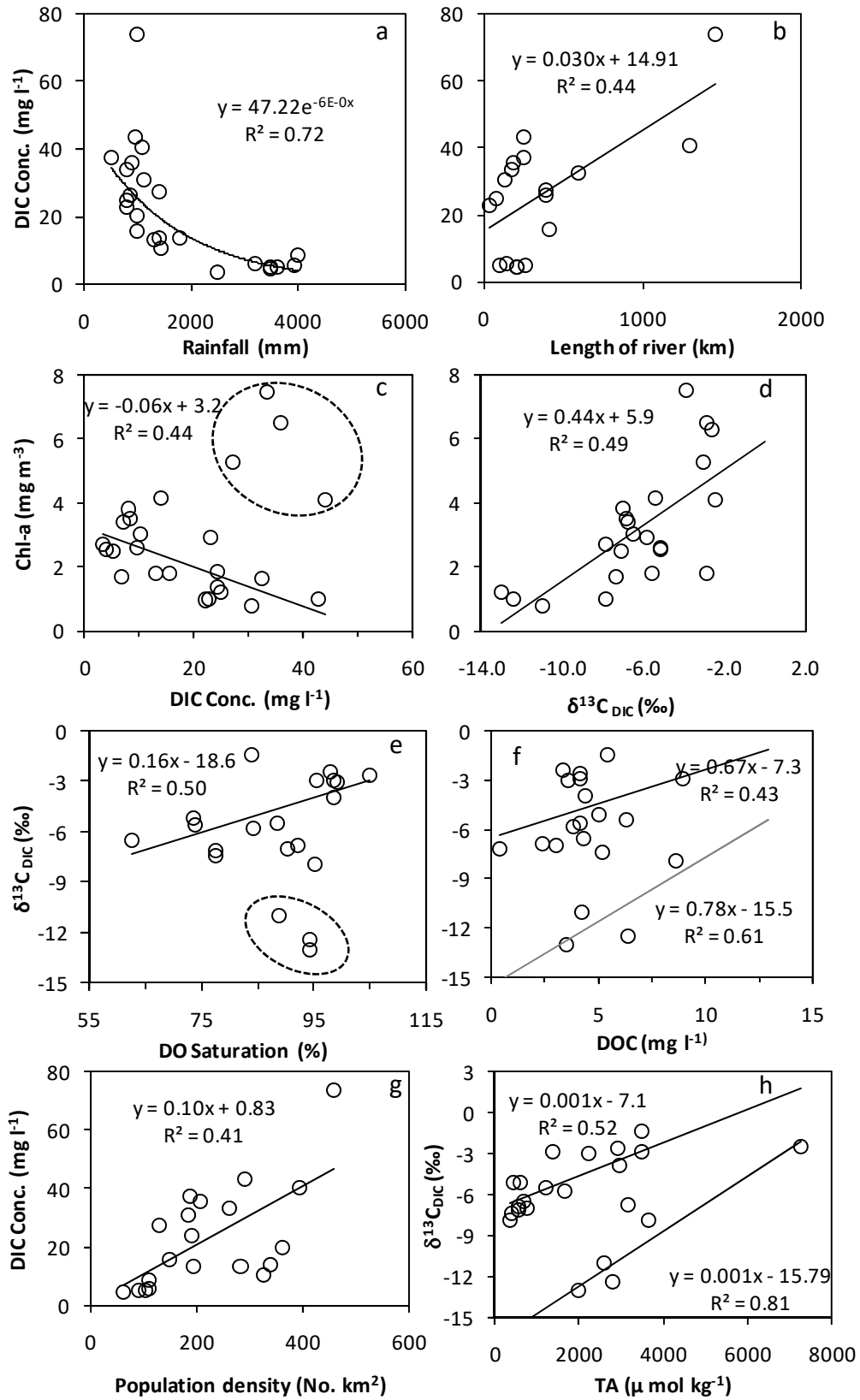


Fig. 4

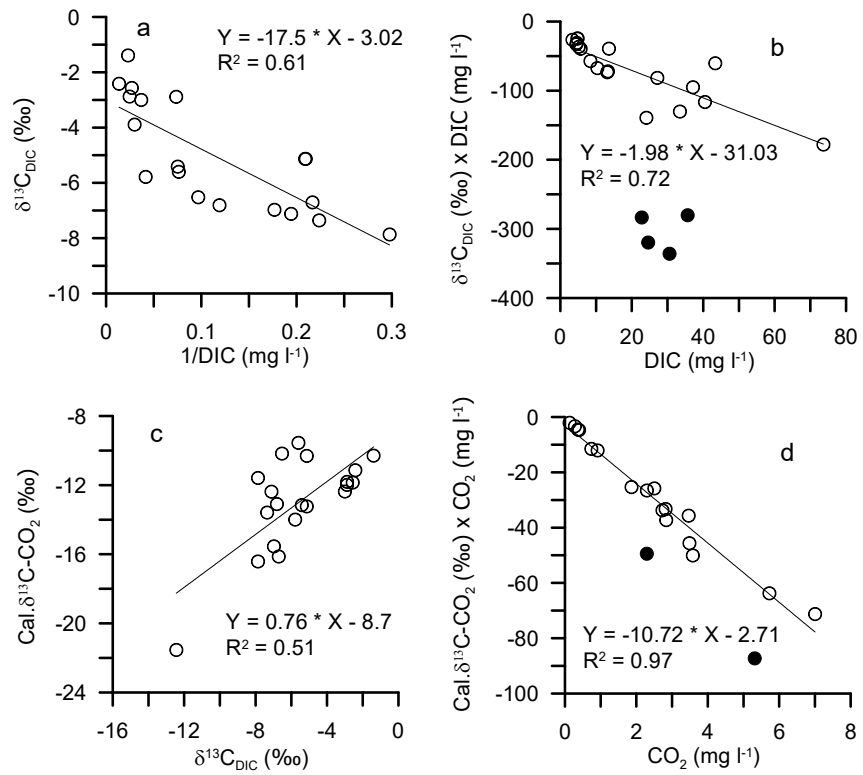


Fig. 5

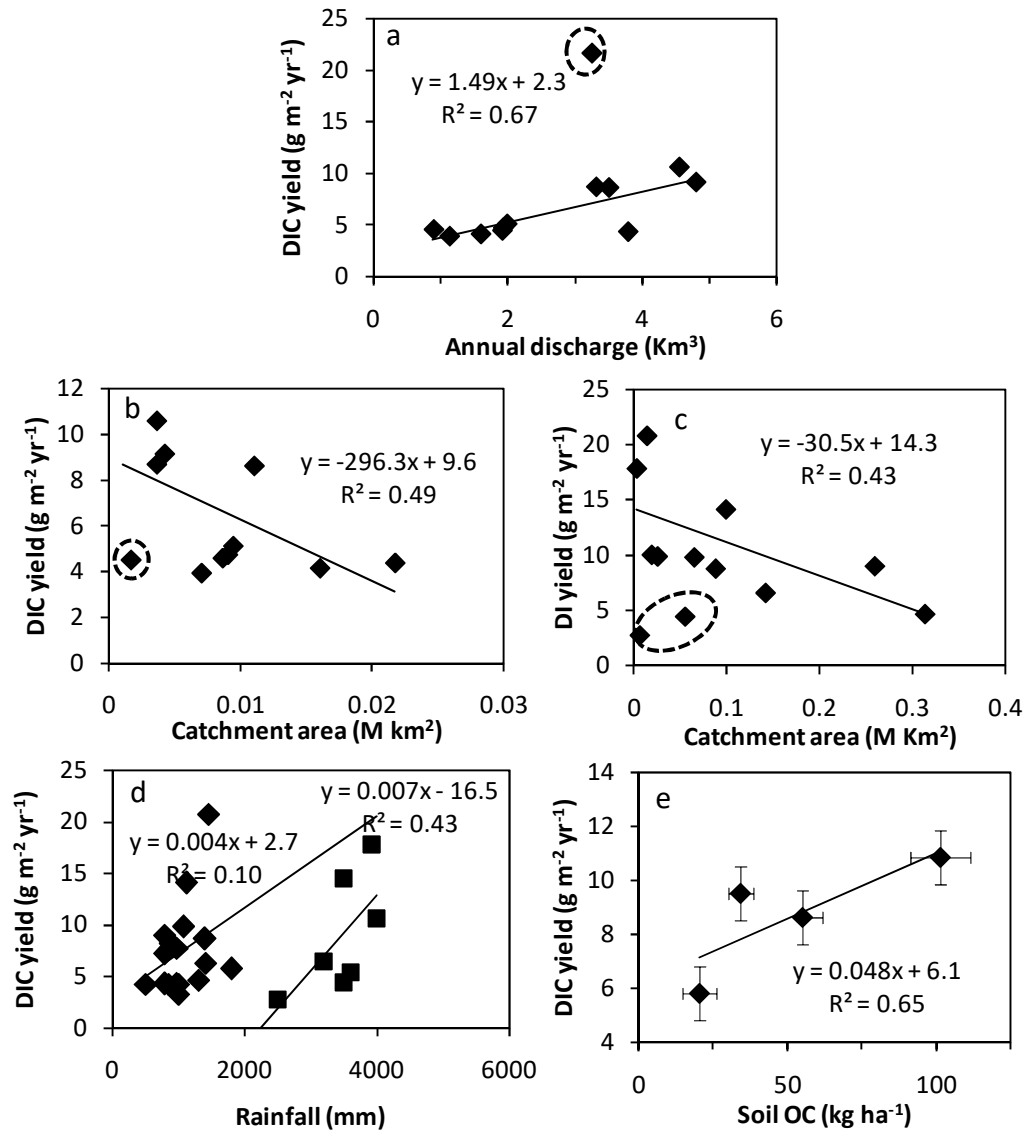


Fig. 6: